

# Photodissociation Dynamics of Propyne and Allene: A View from ab Initio Calculations of the C<sub>3</sub>H<sub>n</sub> (n = 1–4) Species and the Isomerization Mechanism for C<sub>3</sub>H<sub>2</sub>

A. M. Mebel,<sup>\*,†</sup> W. M. Jackson,<sup>\*,†,‡</sup> A. H. H. Chang,<sup>†</sup> and S. H. Lin<sup>†,§,⊥</sup>

Contribution from the Institute of Atomic and Molecular Sciences, Academia Sinica, P.O. Box 23-166, Taipei 10764, Taiwan, ROC, Department of Chemistry, University of California, Davis, California 95616, Department of Chemistry, National Taiwan University, Taipei 106, Taiwan, ROC, and Department of Chemistry and Biochemistry, Arizona State University, Tempe, Arizona 85284-1604

Received August 5, 1997. Revised Manuscript Received April 7, 1998

**Abstract:** Potential energy surfaces of various primary and secondary products from the photodissociation of propyne and allene, including the C<sub>3</sub>H<sub>n</sub> (n = 1–3) species, have been investigated at the CCSD(T)/6-311+G-(3df,2p)//B3LYP/6-311G(d,p) level of theory. The calculated heats of the reactions and the activation barriers for H<sub>2</sub> elimination from C<sub>3</sub>H<sub>n</sub> (n = 2–4) have been employed to analyze the experimental translational energy distribution for different photodissociation channels. The electronic spectra of propyne and various isomers of C<sub>3</sub>H<sub>2</sub> have been calculated by using the CASSCF, MRCI, and EOM-CCSD methods with the ANO(2+) basis set. The calculations suggest that the photodissociation of propyne at 193 nm involves a Franck–Condon transition to the <sup>1</sup>E excited state. After internal conversion into the vibrationally excited ground electronic state, propyne can either dissociate to produce HCCCH + H<sub>2</sub> or isomerize to allene which, in turn, undergoes the H<sub>2</sub> elimination giving H<sub>2</sub>CCC. The HCCCH produced from propyne can have sufficiently high internal energy to rearrange to H<sub>2</sub>CCC. In both mechanisms, the formation of C<sub>3</sub> + H<sub>2</sub> from propyne and allene goes via the same intermediate, which explains the identical rotational distribution of the C<sub>3</sub> products in experiment. The H<sub>2</sub> elimination is a minor channel of propyne photodissociation and the major channel is elimination of the acetylenic hydrogen atom. The rearrangement mechanism of C<sub>3</sub>H<sub>2</sub> in the ground electronic state also has been studied. Automerization of H<sub>2</sub>CCC can take place either via a cyclopropyne transition state (the barrier is 37.5 kcal/mol, ref 18) or through isomerization to cyclopropenylidene and backward via TS6 (the barrier is 41.7 kcal/mol). Isomerization of triplet propargylene to cyclo-C<sub>3</sub>H<sub>2</sub> occurs by the ring closure via the triplet–singlet seam of crossing MSX1, and the activation energy is predicted to be about 41 kcal/mol. Cyclopropenylidene can undergo automerization by the 1,2-H shift via TS10 with the barrier of 32.4 kcal/mol. The direct triplet HCCCH → H<sub>2</sub>CCC isomerization proceeds by the 1,3-hydrogen shift via MSX2 and TS8 or TS9 with a high activation energy of 78–81 kcal/mol. The singlet propargylene can also rearrange to cyclo-C<sub>3</sub>H<sub>2</sub> via TS7 (barrier 37.4 kcal/mol) and to H<sub>2</sub>CCC via TS8 or TS9. The calculated PES for the ground and excited states have allowed us to explain the experimentally observed automerizations and isomerizations of C<sub>3</sub>H<sub>2</sub> isomers and to assign their UV absorption spectra.

## Introduction

There have been substantial efforts in recent years to study and understand the photodissociation dynamics of two isomers of C<sub>3</sub>H<sub>4</sub>, allene and propyne.<sup>1–4</sup> The primary product channels of the allene photodissociation include C<sub>3</sub>H<sub>3</sub> + H and C<sub>3</sub>H<sub>2</sub> + H<sub>2</sub>.<sup>1</sup> The C<sub>3</sub>H<sub>3</sub> and C<sub>3</sub>H<sub>2</sub> molecules undergo secondary photolysis to give various products, such as C<sub>3</sub>H + H<sub>2</sub>, C<sub>3</sub>H<sub>2</sub> + H, and C<sub>2</sub>H<sub>2</sub> + CH for C<sub>3</sub>H<sub>3</sub> and C<sub>3</sub> + H<sub>2</sub>, C<sub>2</sub>H<sub>2</sub> + C, and C<sub>2</sub>H + CH for C<sub>3</sub>H<sub>2</sub>. The C<sub>3</sub>H<sub>4</sub> (hν) → C<sub>3</sub>H<sub>2</sub> + H<sub>2</sub> (hν) → C<sub>3</sub> + 2H<sub>2</sub>

process has been suggested to be responsible for the formation of the C<sub>3</sub> molecules in comets.<sup>3</sup> The highly reactive C<sub>3</sub>H<sub>n</sub> (n = 1–3) molecules and radicals are of fundamental significance for organic chemistry, but they are also thought to be precursors for the formation of soot in flames<sup>5</sup> and the reactants that could lead to unsaturated molecules in the interstellar medium.<sup>6–8</sup>

The laser induced fluorescence (LIF) study of the photodissociation of allene<sup>2</sup> at 193 nm showed that C<sub>3</sub> is produced from C<sub>3</sub>H<sub>2</sub> with very cold rotational distributions in the 000 and 010 states. Although propyne has a geometry and electronic structure, distinctly different from those of allene, it also absorbs at 193 nm and produces C<sub>3</sub> with a rotational population identical to the one observed from allene.<sup>2</sup> To explain this result, one

<sup>†</sup> Academia Sinica.

<sup>‡</sup> University of California.

<sup>§</sup> National Taiwan University.

<sup>⊥</sup> Arizona State University.

(1) Jackson, W. M.; Anex, D. S.; Continetti, R. E.; Lee, Y. T. *J. Chem. Phys.* **1991**, *95*, 7327.

(2) Song, X.; Bao, Y.; Urdahl, R. S.; Gosine, J. N.; Jackson, W. M. *Chem. Phys. Lett.* **1994**, *217*, 216.

(3) Jackson, W. M. In *Comets in the Post-Halley Era*; Newburn, R. L., Ed.; Kluwer Academic Publishers: Amsterdam, 1991; Vol. 1, p 313.

(4) (a) Seki, K.; Okabe, H. *J. Phys. Chem.* **1992**, *96*, 3345. (b) Satyapal, S.; Bersohn, R. *J. Phys. Chem.* **1991**, *95*, 8004.

(5) Slagle, I. R.; Gutman, D. In *Twenty-First Symposium (International) on Combustion*; The Combustion Institute: Pittsburgh, PA, 1986; p 875.

(6) Thaddeus, P.; Vrtilik, J. M.; Gottlieb, C. A. *Astrophys. J.* **1985**, *299*, L63.

(7) Marsden, B. G. *Annu. Rev. Astron. Astrophys.* **1974**, *12*, 1.

(8) Jackson, W. M. In *Laboratory studies of photochemical and spectroscopic phenomena related to comets*, Wilkening, L. L., Ed.; University of Arizona: Tempe, AZ, 1982; p 480.

has to postulate that the two processes pass through a common intermediate at a certain reaction step.

To get a deeper insight into the photodissociation dynamics of allene and propyne, one has to study potential energy surfaces (PES) of various isomers of  $C_3H_4$ ,  $C_3H_3$ ,  $C_3H_2$ , and  $C_3H$  and their isomerization and dissociation channels in the ground and excited states which are accessible with absorption of a 193 nm photon. This determines the broad scope of this paper. The ground-state PES of  $C_3H_4$  is well established.<sup>9–12</sup> For the other species of the series, equilibrium structures have been reported.<sup>13–16</sup> However, their isomerization and dissociation pathways and excited electronic states have not received as much attention by theorists. In the previous work,<sup>17</sup> we studied the electronic spectra of allene and vinylidene carbene ( $H_2CCC$ ) and potential energy surfaces for excited states of these species. We also investigated PES for  $H_2$  elimination from allene. In this paper, we present the results of ab initio calculations of the electronic spectrum of propyne and PES for its various primary and secondary photodissociation products, such as  $C_3H_n$  ( $n = 1–3$ ). We discuss in more detail the isomerization mechanism of  $C_3H_2$  and the electronic spectra of this species.  $C_3H_2$  is the key intermediate in production of  $C_3$  during the photodissociation of propyne and allene. Earlier we found that once  $H_2CCC$  is formed in the primary photodissociation of allene, its most probable internal energy is  $\sim 43$  kcal/mol.<sup>17</sup> HCCCH formed from propyne can also have a high internal energy. Therefore, isomerization of the  $C_3H_2$  species can affect the photodissociation dynamics if the rearrangement barriers are low enough. On the other hand, the isomerization mechanism is interesting itself and was a subject of a recent experimental study by Seburg

et al.<sup>18</sup> After considering the  $C_3H_2$  isomerization, the electronic spectrum is considered because it may be useful for the detection of this radical. Stanton et al.<sup>19</sup> recently published the first experimental absorption spectrum of one of the isomers of  $C_3H_2$ , vinylidene carbene, and interpreted the spectrum using EOM-CCSD calculations.

Possible dissociation channels of  $C_3H_2$  which can occur after absorption of the second photon during the laser photolysis of allene and propyne are also discussed. The results of the PES calculations are applied to understand and compare the photodissociation mechanism of two fundamental geometric isomers of  $C_3H_4$ .

## Methods of Calculations

For the ground electronic state, the geometry of equilibrium structures and transition states of  $C_3H_n$  ( $n = 1–4$ ) have been optimized by using the hybrid density functional B3LYP method<sup>20</sup> and, in some cases, the ab initio MP2<sup>21</sup> or CCSD(T)<sup>22</sup> methods with the 6-311G(d,p) basis set. Vibrational frequencies, calculated at the B3LYP/6-311G(d,p) level, have been used for characterization of the stationary points and zero-point energy (ZPE) correction. To obtain more accurate energies on the ground-state PES we used the CCSD(T) approach with the large 6-311+G(3df,2p) basis set. The CCSD(T)/6-311+G(3df,2p)//B3LYP calculational scheme has been shown<sup>23</sup> to provide accuracies of 1–2 kcal/mol for the atomization energies of the G2 test set of molecules. At the CCSD(T)/6-311+G(3df,2p)//B3LYP/6-311G(d,p) + ZPE[B3LYP/6-311G(d,p)] level, the atomization energy of the  $H_2$  molecule is underestimated by 2.2 kcal/mol. However, we do not use any empirical “higher level correction” in the present study. For the reactions involving a bond fission we expect the calculated energies to be 1–2 kcal/mol lower than the actual values. A similar CCSD(T)//B3LYP approach has also been demonstrated to be accurate for transition state energies.<sup>24</sup> The search for minima on the seam of crossing (MSX) between singlet and triplet PES of  $C_3H_2$  has been performed at the B3LYP/6-311G(d,p) level by using the program written by Cui, Dunn, and Morokuma.<sup>25</sup>

For excited states, geometry optimization of various stationary points has been carried out by using the multireference CASSCF method<sup>26</sup> with the 6-311+G(d,p) basis set. The active space included eight electrons distributed on 10 orbitals, CASSCF(8,10). Vibrational frequencies for the excited-state equilibrium structures have been calculated at the CIS/6-311+G(d,p) level.<sup>27</sup> The energies of excited

(9) Honjou, N.; Pacansky, J.; Yoshimine, M. *J. Am. Chem. Soc.* **1985**, *107*, 5322.

(10) Yoshimine, M.; Pacansky, J.; Honjou, N. *J. Am. Chem. Soc.* **1989**, *111*, 2785.

(11) Yoshimine, M.; Pacansky, J.; Honjou, N. *J. Am. Chem. Soc.* **1989**, *111*, 4198.

(12) Bettinger, H. F.; Schreiner, P. R.; Schleyer, P. v. R.; Schaefer, H. F., III. *J. Phys. Chem.* **1996**, *100*, 16147.

(13) (a) Jahn, H. A.; Teller, E. *Proc. R. Soc. London* **1957**, *A161*, 220.

(b) Gleiter, R.; Hoffmann, R. *J. Am. Chem. Soc.* **1968**, *90*, 5457. (c) Lathan, W. A.; Radom, L.; Hariharan, P. C.; Hehre, W. J.; Pople, J. A. *Top. Curr. Chem.* **1973**, *40*, 1. (d) Hehre, W. J.; Pople, J. A.; Lathan, W. A.; Radom, L.; Wasserman, E.; Wasserman, Z. R. *J. Am. Chem. Soc.* **1976**, *98*, 4378.

(e) Lee, C. K.; Li, W. K. *J. Mol. Struct.* **1977**, *38*, 253. (f) Baird, N. C.; Taylor, K. F. *J. Am. Chem. Soc.* **1978**, *100*, 1333. (g) Kollmar, H. *J. Am. Chem. Soc.* **1978**, *100*, 2660. (h) Kenney, J. W.; Simons, J.; Purvis, G. D.; Bartlett, R. J. *J. Am. Chem. Soc.* **1978**, *100*, 6930. (i) Dykstra, C. E.; Parsons, C. A.; Oates, C. L. *J. Am. Chem. Soc.* **1979**, *101*, 1962. (j) Shepard, R.; Banerjee, A.; Simons, J. *J. Am. Chem. Soc.* **1979**, *101*, 6174. (k) Kühnel, W.; Gey, E.; Spangenberg, H.-J. *Z. Phys. Chem., Leipzig* **1982**, *263*, 641.

(l) Lee, T. J.; Bunge, A.; Schaefer, H. F., III. *J. Am. Chem. Soc.* **1985**, *107*, 137. (m) DeFrees, D. J.; McLean, A. D. *Astrophys. J.* **1986**, *308*, L31. (n) Maier, G.; Reisenauer, H. P.; Schwab, W.; Carsky, P.; Hess, B. A., Jr.; Schaad, L. J. *J. Am. Chem. Soc.* **1987**, *109*, 5183. (o) Cooper, D. L.; Murphy, S. C. *Astrophys. J.* **1988**, *333*, 482. (p) Bofill, J. M.; Farras, J.; Olivella, S.; Sole, A.; Vilarrasa, J. *J. Am. Chem. Soc.* **1988**, *110*, 1694. (q) Fan, Q.; Pfeiffer, G. V. *Chem. Phys. Lett.* **1989**, *162*, 472. (r) Maier, G.; Reisenauer, H. P.; Schwab, W.; Carsky, P.; Spirko, V.; Hess, B. A., Jr.; Schaad, L. J. *J. Chem. Phys.* **1989**, *91*, 4763. (s) Carsky, P.; Spirko, V.; Hess, B. A., Jr.; Schaad, L. J. *J. Phys. Chem.* **1990**, *94*, 5493. (t) Maclagan, R. G. A. R. *J. Mol. Struct. (THEOCHEM)* **1992**, *258*, 175. (u) Jonas, V.; Böhme, M.; Frenking, G. *J. Phys. Chem.* **1992**, *96*, 1640. (v) Gottlieb, C. A.; Killian, T. C.; Thaddeus, P.; Botschwina, P.; Flügge, J.; Oswald, M. *J. Chem. Phys.* **1993**, *98*, 4478. (w) Wong, M. W.; Radom, L. *J. Am. Chem. Soc.* **1993**, *115*, 1507. (x) Botschwina, P.; Horn, M.; Flügge, J.; Seeger, S. *J. Chem. Soc., Faraday Trans.* **1993**, *89*, 2219. (y) Herges, R.; Mebel, A. M. *J. Am. Chem. Soc.* **1994**, *116*, 8229.

(14) (a) Honjou, N.; Yoshimine, M.; Pacansky, J. *J. Phys. Chem.* **1987**, *91*, 4455. (b) Collin, G. J.; Deslauriers, H.; De Maré, G. R.; Poirier, R. D. *J. Phys. Chem.* **1990**, *94*, 134.

(15) Walch, S. P. *J. Chem. Phys.* **1995**, *103*, 7064.

(16) Takahashi, J.; Yamashita, K. *J. Chem. Phys.* **1996**, *104*, 6613.

(17) Jackson, W. M.; Mebel, A. M.; Lin, S. H.; Lee, Y. T. *J. Phys. Chem.* **1997**, *101*, 6638.

(18) Seburg, R. A.; Patterson, J. F.; Stanton, J. F.; McMahon, R. J. *J. Am. Chem. Soc.* **1997**, *119*, 5847.

(19) Stanton, J. F.; DePinto, J. T.; Seburg, R. A.; Hodges, J. A.; McMahon, R. J. *J. Am. Chem. Soc.* **1997**, *119*, 429.

(20) (a) Becke, A. D. *J. Chem. Phys.* **1993**, *98*, 5648. (b) Becke, A. D. *J. Chem. Phys.* **1992**, *96*, 2155. (c) Becke, A. D. *J. Chem. Phys.* **1992**, *97*, 9173. (d) Lee, C.; Yang, W.; Parr, R. G. *Phys. Rev.* **1988**, *B 37*, 785.

(21) For the description of the ab initio methods and the basis sets of the 6-311G(d,p) type see: Hehre, W. J.; Radom, L.; Schleyer, P. v. R.; Pople, J. *Ab Initio Molecular Orbital Theory*; Wiley: New York, 1986.

(22) (a) Purvis, G. D.; Bartlett, R. J. *J. Chem. Phys.* **1982**, *76*, 1910. (b) Scuseria, G. E.; Janssen, C. L.; Schaefer, H. F., III. *J. Chem. Phys.* **1988**, *89*, 7382. (c) Scuseria, G. E.; Schaefer, H. F., III. *J. Chem. Phys.* **1989**, *90*, 3700. (d) Pople, J. A.; Head-Gordon, M.; Raghavachari, K. *J. Chem. Phys.* **1987**, *87*, 5968.

(23) (a) Bauschlicher, C. W., Jr.; Partridge, H. *J. Chem. Phys.* **1995**, *103*, 1788. (b) Bauschlicher, C. W., Jr.; Partridge, H. *Chem. Phys. Lett.* **1995**, *240*, 533.

(24) (a) Mebel, A. M.; Morokuma, K.; Lin, M. C. *J. Chem. Phys.* **1995**, *103*, 7414. (b) Mebel, A. M.; Morokuma, K.; Lin, M. C.; Melius, C. F. *J. Phys. Chem.* **1995**, *99*, 1900. (c) Mebel, A. M.; Morokuma, K.; Lin, M. C. *J. Chem. Phys.* **1995**, *103*, 3440.

(25) Some details of the algorithm for the MSX search have been described in: Dunn, K.; Morokuma, K. *J. Chem. Phys.* **1995**, *102*, 4904. The program uses the HONDO 8.4 package by M. Dupuis.

(26) (a) Werner, H.-J.; Knowles, P. J. *J. Chem. Phys.* **1985**, *82*, 5053. (b) Knowles, P. J.; Werner, H.-J. *Chem. Phys. Lett.* **1985**, *115*, 259.

(27) Foresman, J. B.; Head-Gordon, M.; Pople, J. A.; Frisch, M. J. *J. Phys. Chem.* **1992**, *96*, 135.

**Table 1.** Vertical and Adiabatic Excitation Energies (eV) and Oscillator Strengths for Electronic Transitions of Propyne

state	CASSCF(8,10)/ ANO(2+)	MRCI(4,8)/ ANO(2+)	MRCI+D(4,8)/ ANO(2+)	oscillator strength
<sup>1</sup> E				
vertical	6.60	7.30	7.31	0.0276
adiabatic:				
<sup>1</sup> A'' trans	5.32	5.13	5.01	
cis	5.76	5.62	5.47	
<sup>2</sup> <sup>1</sup> A' trans		6.90	6.62	
cis	6.30	6.07	5.77	
<sup>1</sup> A <sub>2</sub>	7.02	7.72	7.48	0.0
<sup>2</sup> <sup>1</sup> A <sub>1</sub>	7.29	7.94	7.95	0.0413
<sup>2</sup> E	7.76	8.42	8.17	0.0246

state structures were then refined by using internally contracted MRCI<sup>28</sup> calculations. The CASSCF(8,10) wave function was taken as a reference for the MRCI(4,8) computation with the Davidson correction for quadruple excitations (MRCI+D). The basis set used in the MRCI calculations is ANO(2+), i.e., the ANO basis set<sup>29</sup> (4s3p2d for C, 3s2p for H) augmented with several diffuse functions for the carbon atom.<sup>30</sup> The oscillator strengths have been calculated by using the CASSCF transition moments and the MRCI+D energies. For comparison, we have also carried out the equation-of-motion coupled cluster (EOM-CCSD)<sup>31</sup> calculations for the vertical excitation energies.

The MOLPRO-96,<sup>32</sup> GAUSSIAN 94,<sup>33</sup> and ACES-II<sup>34</sup> programs were used for the calculations. The total energies and ZPE corrections as well as vibrational frequencies of the C<sub>3</sub>H<sub>2</sub> species, calculated at various levels of theory, are collected in the Supporting Information.

## Results and Discussion

**Electronic Spectrum of Propyne.** The vertical and adiabatic excitation energies of propyne are shown in Table 1 and the optimized geometries of the ground and excited states are drawn in Figure 1. The simple assumption, often used in the theoretical analysis of electronic spectra, is that "vertical excitation energy" = "absorption maximum". The adiabatic excitation energy should correspond to the origin of the absorption band, i.e., the lowest energy an excited state can absorb if the optical transition occurs from the vibrationless ground state. In principle, the excited state can absorb photons with any energies spaced from the origin by integer numbers of vibrational frequencies of the excited state (in harmonic approximation). The intensity of each vibronic (electronic + vibrational) transition is defined by its Franck-Condon factor. The higher the difference between the photon energy and the adiabatic excitation energy, the more vibrationally excited the molecule should be in the excited electronic state after absorption of the photon.

(28) (a) Werner, H.-J.; Knowles, P. J. *J. Chem. Phys.* **1988**, *89*, 5803. (b) Knowles, P. J.; Werner, H.-J. *Chem. Phys. Lett.* **1988**, *145*, 514.

(29) Widmark, P.-O.; Malmqvist, P.-Å.; Roos, B. O. *Theor. Chim. Acta* **1990**, *77*, 291.

(30) Serrano-Andres, L.; Merchan, M.; Nebot-Gil, I.; Lindh, R.; Roos, B. O. *J. Chem. Phys.* **1993**, *98*, 3151.

(31) Stanton, J. F.; Bartlett, R. J. *J. Chem. Phys.* **1993**, *98*, 7029.

(32) MOLPRO is a package of ab initio programs written by H.-J. Werner and P. J. Knowles, with contributions from J. Almlöf, R. D. Amos, M. J. O. Deegan, S. T. Elbert, C. Hampel, W. Meyer, K. Peterson, R. Pitzer, A. J. Stone, P. R. Taylor, and R. Lindh.

(33) Frisch, M. J.; Trucks, G. W.; Schlegel, H. B.; Gill, P. M. W.; Johnson, B. G.; Robb, M. A.; Cheeseman, J. R.; Keith, T.; Petersson, G. A.; Montgomery, J. A.; Raghavachari, K.; Al-Laham, M. A.; Zakrzewski, V. G.; Ortiz, J. V.; Foresman, J. B.; Cioslowski, J.; Stefanov, B. B.; Nanayakkara, A.; Challacombe, M.; Peng, C. Y.; Ayala, P. Y.; Chen, W.; Wong, M. W.; Andres, J. L.; Replogle, E. S.; Gomperts, R.; Martin, R. L.; Fox, D. J.; Binkley, J. S.; Defrees, D. J.; Baker, J.; Stewart, J. P.; Head-Gordon, M.; Gonzalez, C.; Pople, J. A. GAUSSIAN 94, Revision D.4; Gaussian, Inc.: Pittsburgh, PA, 1995.

(34) Stanton, J. F.; Gauss, J.; Watts, J. D.; Lauderdale, W. J.; Bartlett, R. J. ACES-II, University of Florida, USA.

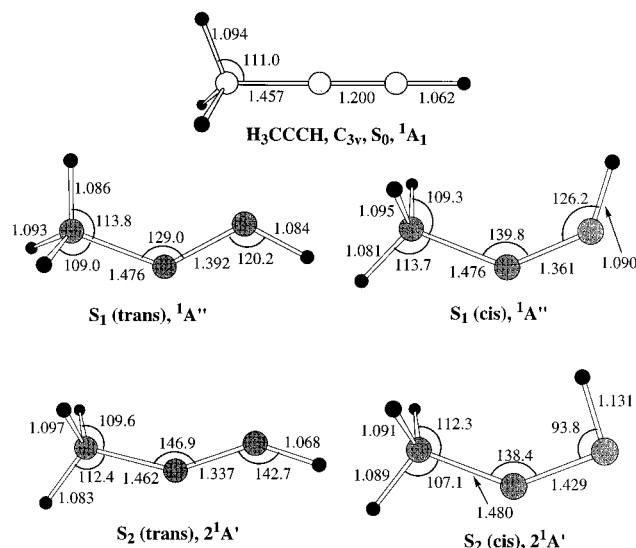


**Figure 1.** Optimized geometry of the ground and excited states of propyne.

Propyne has three singlet states of  $\pi$ - $\pi^*$  character with symmetries of <sup>1</sup>E, <sup>1</sup>A<sub>2</sub>, and <sup>2</sup><sup>1</sup>A<sub>1</sub>. At our best level, MRCI+D/ANO(2+), the vertical excitation energies are 7.31, 7.48, and 7.95 eV, respectively. The next state is <sup>2</sup><sup>1</sup>E ( $\pi$ -3s) with the excitation energy of 8.17 eV. A recent study of Fahr and Nayak showed<sup>35</sup> the maximum in the absorption spectrum of propyne at 7.19 eV, which is close to the vertical excitation energy for <sup>1</sup>E. This state is calculated to have the oscillator strength of ~0.03. The <sup>1</sup>A<sub>1</sub> → <sup>1</sup>A<sub>2</sub> transition is symmetry forbidden, and the oscillator strengths for <sup>2</sup><sup>1</sup>A<sub>1</sub> and <sup>2</sup>E are 0.04 and 0.02, respectively. The excitation energies of propyne are close to those of acetylene.<sup>36,37</sup>

With lowering the symmetry from C<sub>3v</sub> to C<sub>s</sub>, the first excited <sup>1</sup>E state splits into the <sup>2</sup><sup>1</sup>A' and <sup>1</sup>A'' components, both with trans and cis geometries. The geometry optimization for these states gives four minima on PES, shown in Figure 1. The trans and cis forms of the <sup>1</sup>A'' state have adiabatic excitation energies of 5.01 and 5.47 eV, respectively, at the MRCI+D level without ZPE. The geometry is characterized by the bent CCC and CCH groups in the molecule. The acetylenic CC bond is stretched from 1.20 to 1.36–1.39 Å, and the acetylenic CH bond is elongated by 0.02–0.03 Å. There are only small changes in the geometry of the H<sub>3</sub>C–C group. The structures of the CCH group and the adiabatic excitation energies of the trans- and cis-bent <sup>1</sup>A'' are close to those of the trans-<sup>1</sup>A<sub>u</sub> and cis-<sup>1</sup>A<sub>2</sub> states of acetylene,<sup>37b</sup> respectively.

The geometry and energy of the trans-bent minimum on the <sup>2</sup><sup>1</sup>A' surface is similar to the trans <sup>1</sup>B<sub>u</sub> structure of acetylene.<sup>37b</sup> The acetylenic CC bond is stretched to 1.34 Å and the CCC and CCH angles are bent to 143–147°. The elongation of the H<sub>3</sub>CC≡C–H bond is small. The geometry of the cis-bent <sup>2</sup><sup>1</sup>A' minimum is peculiar. The CCH angle reaches 93.8° and the acetylenic CC and CH bonds are stretched to 1.43 and 1.13 Å, respectively. This structure is quite different from that of <sup>1</sup>B<sub>2</sub> for acetylene, earlier reported in the literature.<sup>37b</sup> However, recent calculations of Cui et al.<sup>38</sup> showed that the <sup>1</sup>B<sub>2</sub> structure

(35) Fahr, A.; Nayak, A. *Chem. Phys.* **1996**, *203*, 351.

(36) Robin, M. B. In *Higher Excited States of Polyatomic Molecules*; Academic Press: New York, 1975; Vol. 2.

(37) (a) Peric, M.; Buenker, R.; Peyerimhoff, S. D. *Mol. Phys.* **1984**, *53*, 1177. (b) Peric, M.; Peyerimhoff, S. D.; Buenker, R. *Mol. Phys.* **1987**, *62*, 1339.

(38) Cui, Q.; Morokuma, K.; Stanton, J. F. *Chem. Phys. Lett.* **1996**, *263*, 46.

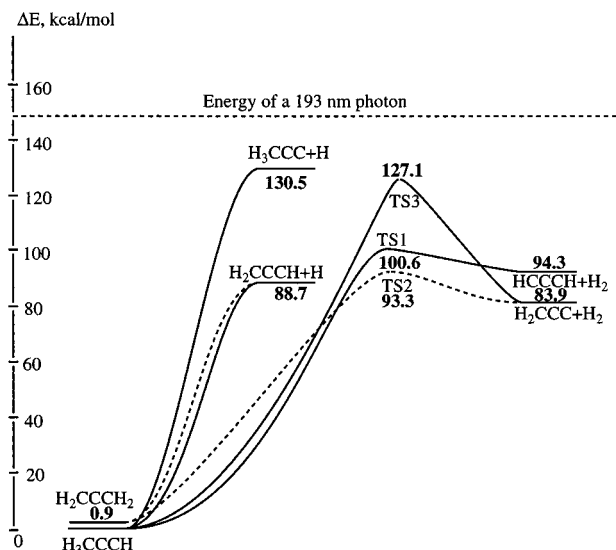
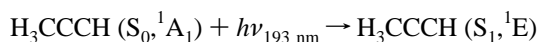


**Figure 2.** Potential energy diagram of primary channels of photodissociation of propyne. Dissociation of allene is shown for comparison by dashed curves. All the energies are calculated at the CCSD(T)/6-311+G(3df,2p)//B3LYP/6-311G(d,p) + ZPE[B3LYP/6-311G(d,p)] level.

for acetylene has two imaginary frequencies. Lowering the symmetry to  $C_s$ , they obtained a *cis*- $C_s$   $2^1A'$  minimum with one strongly bent HCC ( $\sim 90^\circ$ ). The adiabatic excitation energies for the *cis*- $2^1A'$  states of propyne and acetylene are calculated to be 5.77 and 6.22 eV, respectively. Interestingly, Cui et al. found that the *trans*- $1B_u$  structure of acetylene has one imaginary frequency. However, for propyne the corresponding *trans*- $2^1A'$  structure has all real frequencies at the CIS/6-311+G(d,p) level.

The large geometric changes in the  $1A''$  and  $2^1A'$  states lead to large differences between the vertical and adiabatic excitation energies which reach 2.3 eV. Therefore, the vibronic spectrum of propyne corresponding to the  $1A_1 \rightarrow 1E$  transition should be spread over a broad energy region, with small Franck–Condon factors for individual vibronic transitions. Also, the vertical  $1E$  state is correlated to four minima on the  $1A''$  and  $2^1A'$  potential energy surfaces. Therefore, the absorption spectrum should include several overlapping bands. This is consistent with the experiment<sup>35</sup> where the absorption in the region of 6.2–7.5 eV consists of a broad continuum. The second maximum of the absorption band observed at  $\sim 7.4$  eV could be a result of splitting the  $1E$  state. On the other hand, this maximum might be due to the symmetry-forbidden  $1A_2$  state, which borrows some intensity from the allowed transitions because of vibronic coupling.

**Primary Photodissociation Channels of Propyne.** The energetics of various primary channels of propyne photodissociation is shown in Figure 2 and the optimized geometry of different products is presented in Figure 3. The mechanism of photodissociation of propyne at 193 nm involves as the initial step vertical excitation to the  $1E$  state,



The differences between the photon energy and the adiabatic excitation energies of the  $S_1$  ( $1A''$ ) and  $S_2$  ( $2^1A'$ ) equilibrium structures are 0.7–1.4 eV. The normal modes corresponding to the CCC and CCH bending and CH stretching of the acetylenic hydrogen should be excited, while the methyl fragment is not affected. This sheds light on why the elimination of the acetylenic (but not methyl) hydrogen is the major

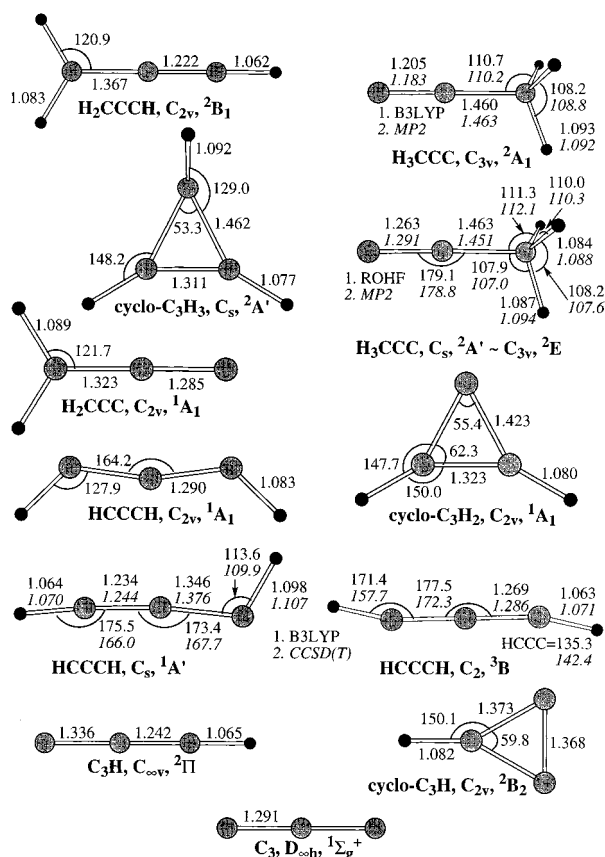


**Figure 3.** Optimized geometry of the equilibrium structures of the  $C_3H_n$  ( $n = 0-3$ ) species, calculated at the B3LYP/6-311G(d,p) level (unless otherwise mentioned).

photodissociation channel,<sup>2,4</sup> although the acetylenic CH bond is much stronger than H–CH<sub>2</sub>CCH. Also, a recent study by Cui et al.<sup>38</sup> showed that the photodissociation mechanism of acetylene involves crossings between the  $S_1$  and  $S_2$ , as well as  $S_2$  and  $S_0$ , surfaces in the energy range of 6.1–6.3 eV along the pathway of the H atom elimination. In view of the similarity of the excited-state surfaces for propyne and acetylene, we expect the fast elimination of the acetylenic hydrogen in H<sub>3</sub>CCCH to occur by a similar mechanism: traveling along the  $S_1$  and  $S_2$  surfaces followed by the  $S_2 \rightarrow S_0$  crossing and elimination of the H atom producing H<sub>3</sub>CCC ( $2A_1$ ).

Experimental measurements by Robinson et al.<sup>39</sup> give the bond dissociation energy (BDE) of  $130.2 \pm 3$  kcal/mol for the acetylenic CH bond in propyne. On the other hand, the MCPF calculations by Bauschlicher and Langhoff<sup>40</sup> resulted in a significantly higher value of  $135.9 \pm 2$  kcal/mol. They found that the ground state of H<sub>3</sub>CCC is  $2E$ , which lies 9.7 kcal/mol below the  $2A_1$  first excited state. When propyne BDE [ $D_0$ -(CH<sub>3</sub>C≡C–H)] is referenced to the  $2A_1$  state, a diabatic BDE is more than 10 kcal/mol higher than the BDE of acetylene ( $131 \pm 0.7$  kcal/mol).<sup>41</sup> For C<sub>2</sub>H, the ground electronic state is of the  $2A_1$  type ( $2\Sigma$ ), but not of  $2E$  ( $2\Pi$ ). Our calculations do not

(39) Robinson, M. S.; Polak, M. L.; Bierbaum, V. M.; DePuy, C. H.; Lineberger, W. C. *J. Am. Chem. Soc.* **1995**, *117*, 6766.

(40) Bauschlicher, C. W., Jr.; Langhoff, S. R. *Chem. Phys. Lett.* **1992**, *193*, 380.

(41) (a) Wodtke, A. M.; Lee, Y. T. *J. Phys. Chem.* **1985**, *89*, 4744. (b) Ervin, K. M.; Gronert, S.; Barlow, S. E.; Gilles, M. K.; Harrison, A. G.; Bierbaum, V. M.; DePuy, C. H.; Lineberger, W. C.; Ellison, G. B. *J. Am. Chem. Soc.* **1990**, *112*, 5750. (c) Baldwin, D. P.; Buntine, M. A.; Chandler, D. W. *J. Chem. Phys.* **1990**, *93*, 6578. (d) Balko, B. A.; Zhang, J.; Lee, Y. T. *J. Chem. Phys.* **1991**, *94*, 7958. (e) Mordaunt, D. H.; Ashfold, M. N. R. *J. Chem. Phys.* **1994**, *101*, 2630.

support the conclusion of Bauschlicher and Langhoff. In the restricted open shell CCSD(T) approximation<sup>32</sup> with the MP2 ZPE correction, the  $^2A_1$  state of  $H_3CCC$  lies 1.0 kcal/mol lower than  $^2E$ .<sup>42</sup> The acetylenic CH bond strength in propyne is then calculated to be 130.5 kcal/mol, in excellent agreement with experiment.<sup>39</sup>

A slower and less probable dissociation mechanism involves internal conversion into the ground state and a redistribution of the energy between vibrational degrees of freedom. Then, propyne can eliminate either a methyl hydrogen or  $H_2$  on the vibrationally excited ground-state surface. The splitting of one of the methyl hydrogens produces the propargyl radical,  $H_2CCCH$ , and is endothermic by 88.7 kcal/mol. The  $H-CH_2-C\equiv CH$  BDE calculated here at the CCSD(T) level is lower than the values suggested by Bauschlicher and Langhoff,<sup>40</sup> 90.5 (MCPF) and  $92.5 \pm 2$  (corrected) kcal/mol. The experimental CH bond strength for methyl hydrogens is  $90.3 \pm 3$  kcal/mol.<sup>39</sup> By comparison, the elimination of a hydrogen atom from allene producing the  $H_2CCCH$  radical is calculated to be endothermic by 87.8 kcal/mol, which is close to the experimental value of 88.7 kcal/mol.<sup>39</sup> The hydrogen atom splitting reactions from propyne and allene have no barrier since the reverse reaction is a radical-radical association.

Two transition states shown in Figure 4 have been found for  $H_2$  elimination from propyne. The reaction pathway via TS1 corresponds to the 1,1- $H_2$  elimination and leads to propargylene,  $HCCCH$ . If the reaction occurs in the singlet manifold, the endothermicity is 94.3 kcal/mol. The barrier height at TS1 is 100.6 kcal/mol. This can be compared with a barrier of 92.4 kcal/mol calculated earlier for the 1,1- $H_2$  elimination from allene.<sup>17</sup> The  $H_2CCCH_2 \rightarrow TS2 \rightarrow H_2CCC + H_2$  reaction was calculated to be endothermic by 83.0 kcal/mol, in close agreement with experiment.<sup>39,43</sup> The reverse barrier for the insertion of  $H_2$  into singlet  $HCCCH$  is 6.3 kcal/mol, or  $\sim 3$  kcal/mol lower than that for the  $H_2$  insertion into  $H_2CCC$  leading to allene via TS2. TS1 is a later transition state than TS2. It has longer CH distances, 1.68 and 2.18 Å, and the HH bond in  $H_2$  is stretched by only 0.04 Å as compared to that in free  $H_2$ . The geometry of the  $HCCCH$  molecular component in TS1 is nearly identical with the geometry of singlet propargylene. The 1,3- $H_2$  elimination occurring via TS3 requires a much higher activation energy. The barrier is 127.1 kcal/mol, while the  $H_3CCCH \rightarrow TS3 \rightarrow H_2CCC + H_2$  reaction is endothermic by 83.9 kcal/mol. Therefore, the barrier for the insertion of  $H_2$  into vinylidencarbene producing propyne is high, 43.2 kcal/mol. The 1,3-insertion of  $H_2$  is not expected to compete with the 1,1-insertion leading to allene. TS3 has a five-member-ring geometry and is a rather early transition state. The forming HH bond is 0.27 Å longer than the regular HH bond in  $H_2$ . The CH distances in the breaking CH bonds are shorter than those in TS1 and TS2. The geometry of the  $H_2CCC$  fragment is quite different from the geometry of propyne and vinylidencarbene. In particular, the CCC angle is strongly bent, but in the reactant

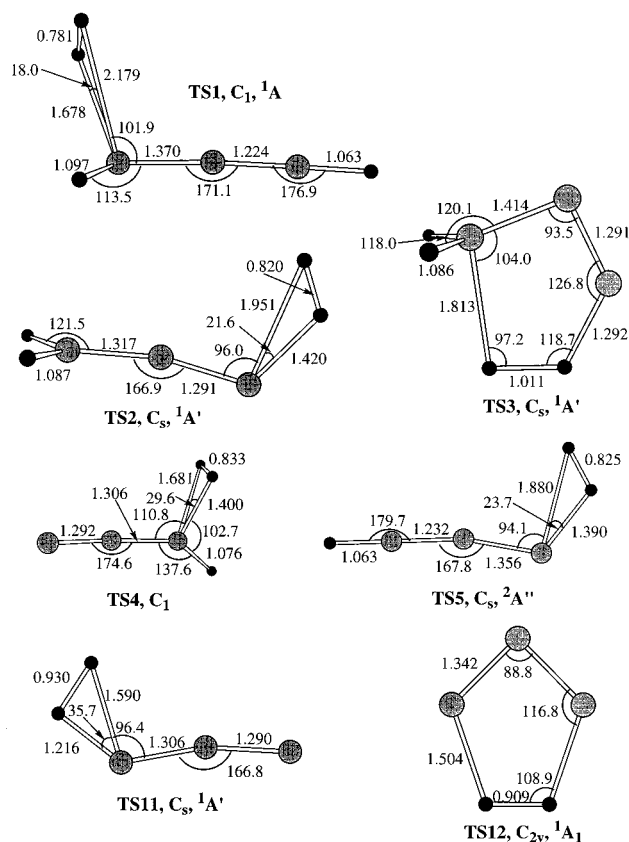


**Figure 4.** B3LYP/6-311G(d,p) optimized geometry of the transition states for  $H_2$  elimination from the  $C_3H_n$  species ( $n = 2-4$ ).

and the final product the CCC group is linear. If the 1,3- $H_2$  elimination from propyne takes place, the dissociation has to proceed via a strongly distorted geometry, which results in a high barrier for this process.

In propyne, the activation energies for the 1,1-elimination of  $H_2$  and a H elimination from the  $CH_3$  carbon atom are 100.6 and 88.7 kcal/mol, respectively. In the combustion of propyne the large energy difference between these two processes leads to CH fission.<sup>44</sup> In the photodissociation of propyne a small amount of  $H_2$  is produced.<sup>2</sup> This can be due to isomerization of propyne to allene followed by  $H_2$  elimination,



The vibrationally excited propyne molecule possesses sufficient energy to overcome the rearrangement barriers.<sup>9-11</sup>

**Secondary Dissociation of  $C_3H_3$ .** The energies of secondary dissociation channels involving  $C_3H_3$  are shown in Figure 5. First we follow the fate of the propyn-1-yl radical,  $H_3CCC$ , the major product of the propyne photodissociation. After absorption of the second photon and internal conversion onto the ground-state surface  $H_3CCC$  can dissociate by three different mechanisms. The most energetically favorable mechanism is fission of a CH bond giving vinylidencarbene,  $H_2CCC$ . The reaction does not have a reverse barrier. The calculated BDE for this process is 54.5 kcal/mol, so the bond in propyn-1-yl is much weaker than the CH bond in the  $CH_3$  group of propyne. Elimination of  $H_2$  from the propyn-1-yl radical proceeds via transition state TS4 and leads to the linear  $HCCCH$ . The theoretical endothermicity and barrier height are 42.7 and 68.0 kcal/mol, respectively. As seen in Figure 4, the character of

(42) Both ROHF and MP2/6-311G(d,p) optimization for the  $^2E$ -like state of  $H_3CCC$  give the geometry which is similar to that obtained in ref 40, but slightly deviates from  $C_{3v}$  symmetry. The symmetry was lowered to  $C_s$  and the  $^2A'$  component was used for the frequency calculations. All the frequencies are real. Geometry optimization of the  $^2A_1$  state at the B3LYP level gives a  $C_s$ -symmetric structure with a slightly bent CCC fragment, while the  $C_{3v}$  structure has two imaginary frequencies of  $e$  symmetry. However, this result is not confirmed by the higher level calculations. At CCSD(T)/6-311+G(3df,2p), the  $C_{3v}$  structure is 1.8 kcal/mol lower in energy than the  $C_s$  one. At the MP2/6-311G(d,p) level, the  $^2A_1$  state has no imaginary frequencies for the  $C_{3v}$  geometry. The bond lengths, optimized for  $^2A_1$  within  $C_{3v}$  symmetry at the B3LYP and MP2 levels, are close.

(43) Clauberg, H.; Minsek, D. W.; Chen, P. *J. Am. Chem. Soc.* **1992**, *114*, 99.

(44) Kiefer, J. H.; Mudipalli, P. S.; Sidhu, S. S.; Kern, R. D.; Jursic, B. S.; Xie, K.; Chen, H. *J. Phys. Chem. A* **1997**, *101*, 4057.

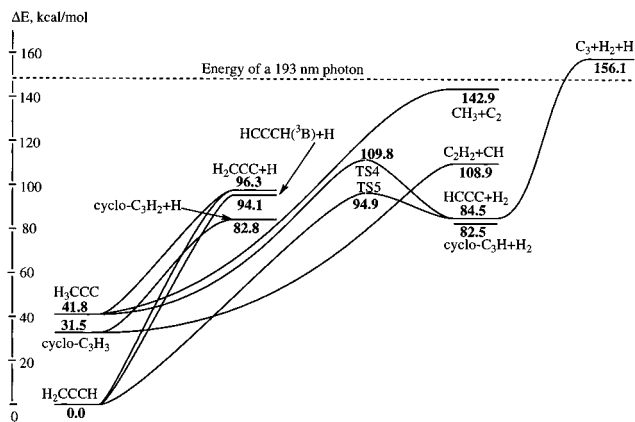


**Figure 5.** Potential energy diagram of the secondary dissociation of  $C_3H_3$ .

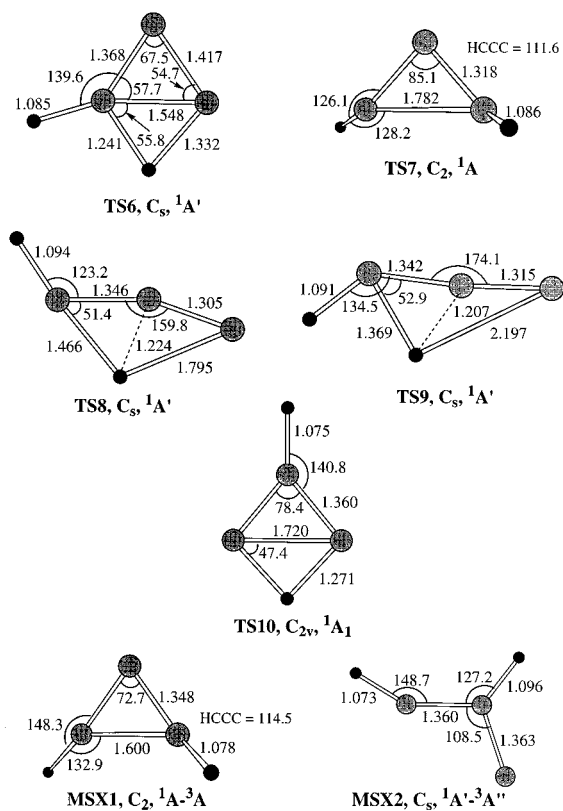


**Figure 6.** B3LYP/6-311G(d,p) optimized geometry of the transition states and minima on the singlet-triplet seam of crossing involved in isomerization of  $C_3H_2$ .

TS4 can be characterized as late, in accordance with endothermicity of the  $H_3CCC \rightarrow HCCC + H_2$  reaction. The propynyl radical can also undergo a cleavage of the single CC bond and produce  $CH_3 + C_2$ . The CC bond dissociation energy is predicted to be 101.1 kcal/mol.

The  $H_2CCCH$  formed as a primary product can absorb a second 193 nm photon<sup>45</sup> and dissociate. Splitting a hydrogen atom from the propargyl radical results either in singlet or triplet propargylene, with an endothermicity of 106.7 (94.1) kcal/mol because of the 12.6 kcal/mol splitting between these two states (see Figure 7). Vinylidene carbene ( $H_2C=C=C:$ ) can also be formed with an endothermicity of 96.3 kcal/mol. The C-H bond dissociation energy,  $D_0(CH_2=C=C-H)$ , measured ex-

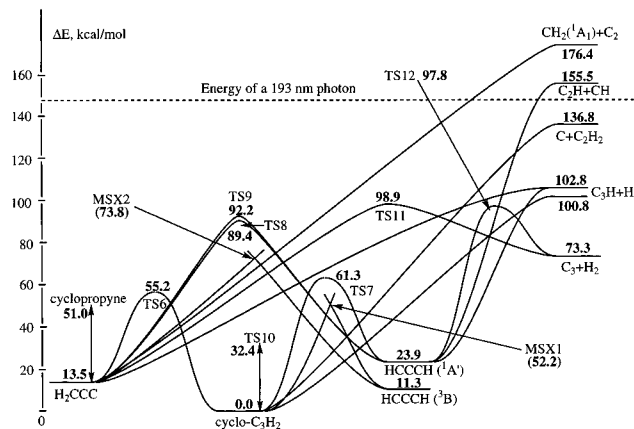


**Figure 7.** Potential energy diagram for isomerization and dissociation of  $C_3H_2$ . The energies are calculated at the CCSD(T)/6-311+G(3df,2p)/B3LYP/6-311G(d,p) + ZPE[B3LYP/6-311G(d,p)] level. The energies of MSX1 and MSX2 (numbers in parentheses) are calculated at the B3LYP/6-311G(d,p) level.

perimentally by Robinson et al., is  $100 \pm 5$  kcal/mol.<sup>39</sup> Our theoretical result lies within the error bars of the experimental value. Both reactions of hydrogen elimination from propargyl leading to singlet  $C_3H_2$  might have a barrier because the reverse reactions involve a radical and a closed shell species. However, the search of transition states in both cases leads to the dissociation of a hydrogen. This means that the reverse reactions of H addition to the singlet HCCC and  $H_2CCC$  have no barrier. These results can be attributed to the high exothermicity of the hydrogen addition.

The propargyl radical can undergo the 1,1- $H_2$  elimination leading to the linear  $C_3H$  structure. The calculated heat of the  $H_2CCCH \rightarrow TS5 \rightarrow HCCC(^2\Pi) + H_2$  reaction is 84.5 kcal/mol. The barrier height is 94.9 and 10.4 kcal/mol with respect to the reactant and products, respectively. In the experiment,  $C_3H_2 + H$ , not  $C_3H + H_2$ , are the major products (96%) of the  $H_2CCCH$  secondary photodissociation.<sup>1</sup> The reason for that is not clear yet because the energies required for the  $H_2$  and H elimination differ by less than 2 kcal/mol. Considering the reverse reactions of 1,1-insertion of  $H_2$  into HCCC, the barrier to form  $H_2CCCH$  is much lower than that to form  $H_3CCC$ . With respect to HCCC +  $H_2$ , TS4 is a later transition state than TS5, with a longer breaking HH bond and shorter forming CH bonds.

The geometry of TS5 is quite similar to that of TS2, the transition state for the 1,1- $H_2$  elimination from allene. In both structures, the  $H_2$  fragment is stretched by  $\sim 0.08$  Å as compared to the free  $H_2$ . The CCC fragment is bent to  $167$ – $168^\circ$  and the breaking CH distances differ from each other. In TS5, the CH distances are slightly shorter than in TS2, 1.39 vs 1.42 and 1.88 vs 1.95 Å. Thus, TS5 is a slightly earlier transition state than TS2. The 1,1- $H_2$  elimination from propargyl is 1.5 kcal/mol more endothermic than that from allene, and the barrier at TS5 is 2.5 kcal/mol higher than that at TS2. For the reverse reactions, the insertion of  $H_2$  into  $C_3H(^2\Pi)$  has an activation energy  $\sim 1$  kcal/mol higher than the activation energy for the corresponding  $H_2$  insertion into vinylidene carbene. Despite the small differences discussed above, the reactions of  $H_2$  elimination from allene and propargyl are very similar according to their energetics and the character of the transition states. Similar to the case of allene, a transition state for 1,3- $H_2$  elimination from  $H_2CCCH$  does not exist.

A third isomer of  $C_3H_3$ , cyclopropenyl ( $C_3,^2A'$ ), is also known.<sup>14a</sup> The cyclic structure is 31.5 kcal/mol less stable than propargyl but 10.3 kcal/mol more stable than  $H_3CCC$ . We could

(45) Fahr, A.; Hassanzadeh, P.; Laszlo, B.; Huie, R. E. *Chem. Phys.* **1997**, *215*, 59.

not find a transition state for H<sub>2</sub> elimination from the cyclopropenyl isomer of C<sub>3</sub>H<sub>3</sub> leading to the cyclic C<sub>3</sub>H. The saddle point search instead results in elimination of a hydrogen atom and formation of cyclopropenylidene C<sub>3</sub>H<sub>2</sub>. The calculated CH bond strength in cyclopropenyl is 51.3 kcal/mol. This value is in satisfactory agreement with the reliable CBS-QCI/APNO result (53.7 kcal/mol) of Montgomery et al.<sup>46</sup> The molecular hydrogen elimination from cyclopropenyl is expected to proceed by a multistep mechanism involving initial isomerization to H<sub>2</sub>-CCCH, eventually leading to linear HCCC. The details of this mechanism are yet to be studied, although some steps have been investigated by Walch.<sup>15</sup> The overall endothermicity of the pathway from cyclic C<sub>3</sub>H<sub>3</sub> to linear HCCC is 53.0 kcal/mol. Among other dissociation channels of C<sub>3</sub>H<sub>3</sub>, the cyclopropenyl isomer can split into CH + C<sub>2</sub>H<sub>2</sub>, which requires an energy of 77.4 kcal/mol. For propargyl, the dissociation to CH (<sup>2</sup>Π) + C<sub>2</sub>H<sub>2</sub> (acetylene) is endothermic by 108.9 kcal/mol and is not likely to occur in one step. One two-step process requires the H<sub>2</sub>CCCH first to rearrange to the cyclopropenyl structure and then to eliminate CH. Another is dissociation to H<sub>2</sub>CC (vinylidene) + CH with the former isomerizing to acetylene.

**Isomerization of C<sub>3</sub>H<sub>2</sub>.** Although the structure and stability of various isomers of C<sub>3</sub>H<sub>2</sub> in the singlet and triplet electronic states has been well studied theoretically,<sup>13</sup> PES for the isomerization pathways is much less investigated by theorists. Kaiser et al.<sup>47</sup> as well as Takahashi and Yamashita<sup>16</sup> have studied PES for the C(<sup>3</sup>P) + C<sub>2</sub>H<sub>2</sub> reaction and calculated some transition states for the isomerization of C<sub>3</sub>H<sub>2</sub> in the triplet state. Takahashi and Yamashita also considered crossing between the singlet and triplet surfaces which can be involved in the rearrangement of singlet cyclopropenylidene to triplet propargylene. Seburg et al.<sup>18</sup> have theoretically studied the automerization of singlet vinylidenecarbene, which proceeds via a planar cyclopropyne transition state. The automerization barrier was calculated to be 37.5 kcal/mol at the CCSD(T)/cc-pVTZ level.

Here, we consider various isomerization pathways of C<sub>3</sub>H<sub>2</sub>. Optimized geometries of different isomers and transition states are shown in Figures 3 and 6, respectively. Note that the B3LYP/6-311G(d,p) geometry of the equilibrium structures is similar to that previously reported in the literature<sup>13</sup> and, in particular, is close to that obtained by Seburg et al. at the CCSD(T)/cc-pVTZ level.<sup>18</sup> The only more problematic case is the singlet HCCCH isomer. The B3LYP calculations give for the C<sub>s</sub> geometry one imaginary frequency, while two minima at this level of theory have C<sub>2v</sub> and C<sub>2h</sub> symmetries. The energy difference between the C<sub>s</sub> and C<sub>2v</sub> structures is very small, 0.4 kcal/mol at the B3LYP level with ZPE correction. However, the CCSD(T)/6-311+G(3df,2p) calculations have reversed the order of stability: the C<sub>s</sub> structure becomes 0.6 kcal/mol more favorable than the C<sub>2v</sub> one. Therefore, we re-optimized the geometry of the C<sub>s</sub>-symmetric singlet propargylene at the CCSD(T)/6-311G(d,p) level. All frequencies at CCSD(T) are real for the C<sub>s</sub> structure, which agrees with the earlier result of Byun and Stanton.<sup>48</sup> For triplet propargylene, the B3LYP calculation gives the correct symmetry for the equilibrium structure, (<sup>3</sup>B,C<sub>2</sub>).<sup>13y</sup> However, the difference between the B3LYP and CCSD(T) geometric parameters is significant, for instance, for the CCH bond angle and the CCCH dihedral angle.

(46) Montgomery, J. A., Jr.; Ochterski, J. W.; Petersson, G. A. *J. Chem. Phys.* **1994**, *101*, 5900.

(47) (a) Kaiser, R. I.; Ochsenfeld, C.; Head-Gordon, M.; Lee, Y. T.; Suits, A. G. *Science* **1996**, *274*, 1508. (b) Kaiser, R. I.; Ochsenfeld, C.; Head-Gordon, M.; Lee, Y. T.; Suits, A. G. *J. Chem. Phys.* **1997**, *106*, 1729. (c) Ochsenfeld, C.; Kaiser, R. I.; Lee, Y. T.; Suits, A. G.; Head-Gordon, M. *J. Chem. Phys.* **1997**, *106*, 4141.

(48) Byun, K. S.; Stanton, J. F. Private communications.

The calculated energy differences between the isomers are also in line with theoretical and experimental literature data.<sup>13,39,43</sup> Cyclopropenylidene is the most stable singlet isomer, while vinylidenecarbene and propargylene lie 13.5 and 23.9 kcal/mol higher in energy, respectively. Triplet propargylene is 2.2 kcal/mol more stable than the singlet H<sub>2</sub>CCC but lies 11.3 kcal/mol higher in energy than singlet cyclopropenylidene.

The potential energy surface for C<sub>3</sub>H<sub>2</sub> isomerization and dissociation is presented in Figure 7. The cyclic structure rearranges to H<sub>2</sub>CCC via transition state TS6. The calculated barrier is 55.2 and 41.7 kcal/mol relative to cyclopropenylidene and vinylidenecarbene, respectively. The ring opening–closure in TS6 is accompanied by a hydrogen shift. The hydrogen shift is a 1,3-H shift with respect to H<sub>2</sub>CCC and a 1,2-H shift with respect to the cyclic isomer. The TS6 has C<sub>s</sub> symmetry and is quite different from both the reactant and the product. The structure of the C<sub>3</sub> group in TS6 is closer to that in cyclopropenylidene.

Isomerization of cyclopropenylidene to the singlet HCCCH occurs by a simple ring opening. The corresponding transition state TS7 has C<sub>2</sub> symmetry and the <sup>1</sup>A electronic state. In TS7, the double (H)C=C(H) bond loses its double character and starts to break apart (1.73 Å). Interestingly, on the B3LYP potential energy surface, TS7 connects two minima of C<sub>2v</sub> symmetry, cyclopropenylidene and the C<sub>2v</sub> structure of HCCCH, which is slightly lower in energy than the C<sub>s</sub> structure. The valence orbital occupation is 3a<sub>1</sub><sup>2</sup>2b<sub>2</sub><sup>2</sup>4a<sub>1</sub><sup>2</sup>5a<sub>1</sub><sup>2</sup>1b<sub>1</sub><sup>2</sup>3b<sub>2</sub><sup>2</sup>6a<sub>1</sub><sup>2</sup> in cyclo-C<sub>3</sub>H<sub>2</sub> vs 3a<sub>1</sub><sup>2</sup>2b<sub>2</sub><sup>2</sup>4a<sub>1</sub><sup>2</sup>3b<sub>2</sub><sup>2</sup>1b<sub>1</sub><sup>2</sup>5a<sub>1</sub><sup>2</sup>4b<sub>2</sub><sup>2</sup> in HCCCH. Therefore, the interconversion between the two isomers should occur with the break of C<sub>2v</sub> symmetry. The transition state structure substantially deviates from the planarity; the HCCC dihedral angle in TS7 is 111.6°. The barrier at TS7 is higher than that at TS6, 61.3 and 37.4 kcal/mol relative to the cyclic and linear isomers, respectively. Thus, the rearrangement of cyclopropenylidene to propargylene should be slower than that to vinylidenecarbene.

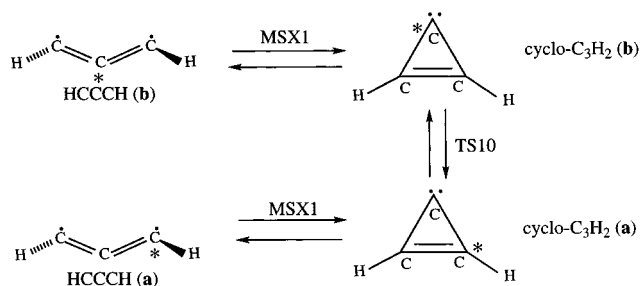
The transformation of H<sub>2</sub>CCC to HCCCH requires a higher activation energy. We have found two transition states separating the two isomers. Both of them, TS8 and TS9, correspond to a 1,3-hydrogen shift. The barrier at TS8, 75.9 kcal/mol relative to vinylidenecarbene, is lower than that at TS9, 78.7 kcal/mol. The geometries of the C<sub>3</sub> fragment are similar in the two transition states, with a stronger CCC bending in TS8. The positions of the hydrogen atoms differ. In TS8, the HCCC fragment containing the moving hydrogen has a cis geometry and the second HCCC has a trans geometry. In TS9, both hydrogens are in trans positions relative to CCC. According to the position of the moving H atom, TS8 has a later character than TS9, if H<sub>2</sub>CCC is considered as the reactant. The intrinsic reaction coordinate (IRC)<sup>49</sup> calculations for TS8 and TS9 confirmed that the two transition states indeed connect H<sub>2</sub>CCC and HCCCH. No HCC(H)C or propenediylidene isomer exists on the singlet PES. Upon geometry optimization, such structures spontaneously rearrange to the other isomers depending on the initial geometry. Propenediylidene is an equilibrium structure only in the triplet electronic state.<sup>16,47</sup>

Thermal automerization of the cyclic C<sub>3</sub>H<sub>2</sub> occurs by the 1,2-H shift via TS10. The barrier is 32.4 kcal/mol, which is lower than the barriers for the rearrangement of this isomer to H<sub>2</sub>CCC and HCCCH as well as the automerization barrier of vinylidenecarbene.

In an elegant experimental study with the <sup>13</sup>C isotope labeled C<sub>3</sub>H<sub>2</sub>, Seburg et al.<sup>18</sup> have investigated the photochemical isomerizations and automerizations of this species. Although

(49) Gonzalez, C.; Schlegel, H. B. *J. Chem. Phys.* **1989**, *90*, 2154.

## Scheme 1



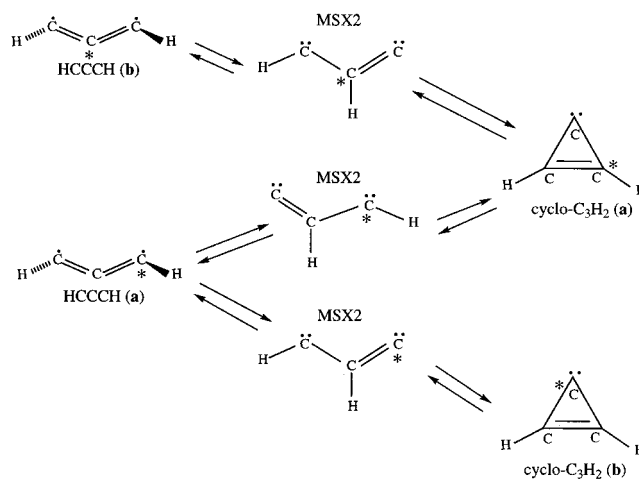
photoexcitation puts  $C_3H_2$  into excited electronic states, the products of the photochemical process are the ground-state isomers, indicating that internal conversion occurs to the ground electronic state. Comparison of the experimental data with the calculated ground-state PES clarifies the rearrangement mechanisms. At  $\lambda > 444$  nm ( $<64.4$  kcal/mol), Seburg et al. observed automerization of vinylidencarbene. They concluded that the reaction proceeds via the cyclopropyne transition state with the barrier of 37.5 kcal/mol. The automerization involving cyclopropenylidene as an intermediate is not consistent with the experimental data on the  $^{13}C$  isotope scrambling. Indeed, the calculated barrier for the  $H_2CCC \leftrightarrow TS6 \leftrightarrow$  cyclopropenylidene  $\leftrightarrow TS6 \leftrightarrow H_2CCC$  automerization is 41.7, 4.2 kcal/mol higher than the barrier at cyclopropyne.

Isomerization of the triplet HCCCH requires not only geometrical changes, such as hydrogen shifts and ring closure, but also an intersystem crossing of the singlet and triplet PES. Hence, we searched for the minimal energy points on the singlet–triplet seam of crossing. MSX1 is such a point on the pathway corresponding to the ring closure between HCCCH and cyclic  $C_3H_2$ .<sup>50</sup> The energy of MSX1 is 52.2 kcal/mol relative to singlet cyclopropenylidene at the B3LYP/6-311G-(d,p) level. At this level, the energy of MSX1 is 12.0 kcal/mol lower than that of TS7, the transition state for the ring closure in the singlet state. According to the geometry of MSX1, shown in Figure 6, in particular, the CCC angle of  $72.7^\circ$  vs  $85.1^\circ$  in TS9, the crossing occurs *after* TS7, if the system travels from HCCCH to cyclopropenylidene. Thus, starting from triplet propargylene the reaction proceeds along the triplet PES, crosses over to the singlet surface, and leads to the singlet cyclic  $C_3H_2$  without going over the barrier at TS7.

The simple ring closure in HCCCH does not explain the experimental observations of the isotope scrambling by Seburg et al., illustrated in Scheme 1 where  $^{13}C$  is marked by “\*”. They found that both isotopomers of cyclopropenylidene can be formed from each isotopomer of propargylene. Also, the second propargylene isotopomer HCCCH (b) or HCCCH (a), respectively, appears immediately upon photolysis of HCCCH (a) or HCCCH (b). To explain this, Seburg et al. suggested that the ring closure is followed by a rapid 1,2-hydrogen shift in cyclopropenylidene. Our findings support the mechanism shown in Scheme 1; the automerization barrier in the cyclo- $C_3H_2$  is relatively low.

The alternative isomerization scenario involves the hydrogen migration in concert with or preceding ring closure, as illustrated in Scheme 2. Hence, we have also optimized the geometry of

## Scheme 2



MSX2, the minimum on the seam of crossing in the vicinity of transient propenediylidene. The crossing takes place at the energy of 66.4 kcal/mol (B3LYP) relative to the triplet HCCCH, more than 20 kcal/mol higher than the energy of MSX1. MSX2 is also higher in energy than TS7. Therefore, after clearing the crossing point, singlet cyclopropenylidene can be formed. The mechanism of the HCCCH ( $^3B$ )  $\leftrightarrow$  cyclo- $C_3H_2$  ( $^1A_1$ ) isomerization involving MSX2 cannot be completely ruled out because the energy of MSX2 is below 91.4 kcal/mol available at  $\lambda = 313$  nm. However, this mechanism is much less favorable than the one involving MSX1 and 1,2-hydrogen shifts in cyclopropenylidene. The mechanism involving MSX2 is inconsistent with experimental data. It predicts that HCCCH (a) should initially produce cyclo- $C_3H_2$  (a) and (b) in a 1:1 ratio and that HCCCH (b) should initially produce only cyclo- $C_3H_2$  (a), which is not the case in the experiment.<sup>18</sup>

MSX2 also can be relevant to the formation of  $H_2CCC$  from the triplet HCCCH at  $\lambda = 313$  nm. The isomerization occurs via the seam of crossing and then via transition states TS8 and TS9. The available energy is sufficient to overcome the barriers for the 1,3-hydrogen shift. The slow rate of reaction for the HCCCH  $\leftrightarrow$   $H_2CCC$  interconversion as compared to HCCCH  $\leftrightarrow$  cyclo- $C_3H_2$  is due to the high energies of the transition states for the 1,3-hydrogen migration.

**Electronic and Vibronic Spectra of  $C_3H_2$ . (a) Vinylidencarbene.** We considered the vertical and adiabatic excitation energies (Table 2) as well as the optimized geometry of excited states (Figure 8) of  $H_2CCC$  in the previous paper.<sup>17</sup> Stanton et al.<sup>19</sup> reported a more resolved absorption spectrum of vinylidencarbene in the region between 200 and 800 nm and interpreted the spectrum using EOM-CCSD calculations. Two states,  $^1B_1$  and  $2^1A_1$ , can contribute to the spectrum. The first excited state of  $H_2CCC$ ,  $^1A_2$ , is symmetry-forbidden. Therefore, only weak absorption may be observed in the region of 1.77–1.88 eV (700–660 nm). Indeed, Stanton et al.<sup>19</sup> reported a weak absorption band originating at 717 nm (1.73 eV). The absorption bands in the 400–600 and 200–250 nm region correspond to the  $^1B_1$  and  $2^1A_1$  states, respectively, with the vertical excitation energies of 2.44 eV (508 nm) and 5.39 eV (230 nm). In accordance with experimentally observed intensities, the calculated oscillator strength of  $^1B_1$  is 4.7 times smaller than that of  $2^1A_1$ .

To carry out a more detailed comparison between the experimental and theoretical spectra, we calculated vibronic spectra for  $^1B_1$  and  $2^1A_1$ . We used the ab initio approach to compute vibrational overlap integrals and Franck–Condon

(50) MSX1 has a  $C_2$ -symmetric geometry and the crossing occurs between the  $^1A$  and  $^3A$  electronic states. The ground state of the triplet  $C_2$ -symmetric HCCCH is  $^3B$ . At the geometry of MSX1,  $^3A$  is the lowest triplet state, while  $^3B$  lies 61.0 kcal/mol higher at the MP2/6-311G(d,p) level. Thus, the  $^3A$  state of MSX1 must correlate with the  $^3B$  ground state of propargylene and the reaction pathway between them should go through nonsymmetric geometry.

**Table 2.** Vertical and Adiabatic Excitation Energies (eV) and Oscillator Strengths for Electronic Transitions of C<sub>3</sub>H<sub>2</sub>

state	MRCI(4,8)/ANO(2+)	MRCI+D(4,8)/ANO(2+)	oscillator strength	EOM-CCSD/ANO(2+)	oscillator strength
H <sub>2</sub> CCC <sup>a</sup>					
<sup>1</sup> A <sub>2</sub> , vert	1.88	1.88	0.0	1.96	0.0
adiabatic	1.76	1.77			
<sup>1</sup> B <sub>1</sub> , vert	2.73	2.44	0.0160	2.80	0.0087
adiabatic	2.12	2.05			
<sup>2</sup> <sup>1</sup> A <sub>1</sub> , vert	5.57	5.39	0.0749	5.57	0.1597
adiabatic	5.12	4.92			
<sup>3</sup> <sup>1</sup> A <sub>1</sub> , vert	6.27	5.80	0.0461	7.47	0.0401
adiabatic	5.75	5.43			
<sup>1</sup> B <sub>2</sub> , vert	5.92	5.84	0.0002	7.11	0.0083
adiabatic	5.80	5.82			
<sup>2</sup> <sup>1</sup> A <sub>2</sub> , vert	6.67	6.58	0.0	7.80	0.0
adiabatic	5.88	5.81			
<sup>2</sup> <sup>1</sup> B <sub>2</sub>				7.49	0.0499
<sup>4</sup> <sup>1</sup> A <sub>1</sub>				7.97	0.2117
<sup>2</sup> <sup>1</sup> B <sub>1</sub>				8.16	0.0303
<sup>3</sup> <sup>1</sup> B <sub>2</sub>				8.24	0.0524
<sup>3</sup> <sup>1</sup> A <sub>2</sub>				8.40	0.0
<sup>5</sup> <sup>1</sup> A <sub>1</sub>				8.42	0.0893
<sup>4</sup> <sup>1</sup> A <sub>2</sub>				8.53	0.0
<sup>4</sup> <sup>1</sup> B <sub>2</sub>				8.57	0.0012
<sup>3</sup> <sup>1</sup> B <sub>1</sub>				8.63	0.0006
<sup>4</sup> <sup>1</sup> B <sub>1</sub>				8.86	0.0819
HCCCH, singlets <sup>b</sup>					
<sup>1</sup> A'', vert	1.30	1.14	0.0026	1.17	0.0018
adiabatic	0.52	0.37			
<sup>2</sup> <sup>1</sup> A', vert	2.83	2.79	0.0017	4.69	0.0114
adiabatic	1.21	1.00			
<sup>2</sup> <sup>1</sup> A'', vert	3.76	3.32	0.0005	4.01	0.0015
adiabatic	3.31	3.05			
<sup>3</sup> <sup>1</sup> A'	5.89	5.68	0.0192	5.78	0.0141
<sup>3</sup> <sup>1</sup> A''	6.52	6.14	0.0038	6.30	0.0040
<sup>4</sup> <sup>1</sup> A'	6.63	6.33	0.0028	5.89	0.0009
<sup>5</sup> <sup>1</sup> A'	6.61	6.38	0.0427	6.51	0.0232
<sup>4</sup> <sup>1</sup> A''	7.33		0.0007	7.04	0.0004
<sup>5</sup> <sup>1</sup> A''				7.30	0.0050
HCCCH, triplets <sup>c</sup>					
<sup>1</sup> <sup>3</sup> A, vert	4.08	4.10	0.0169	4.42	0.0003
adiabatic	3.24	3.28			
<sup>2</sup> <sup>3</sup> B, vert	4.10	4.33	0.0004	4.19	0.0089
adiabatic	3.03	3.02			
<sup>2</sup> <sup>3</sup> A, vert	6.15	5.41	0.0019	4.69	4.6 × 10 <sup>-6</sup>
adiabatic	6.01	5.11		4.41	
<sup>3</sup> <sup>3</sup> B	5.72	5.59	2.8 × 10 <sup>-5</sup>	4.42	0.0003
<sup>4</sup> <sup>3</sup> B	6.76		3.9 × 10 <sup>-5</sup>	5.95	0.0036
<sup>3</sup> <sup>3</sup> A				5.84	7.7 × 10 <sup>-5</sup>
cyclo-C <sub>3</sub> H <sub>2</sub> <sup>d</sup>					
<sup>1</sup> A <sub>2</sub> , vert	4.24	3.92	0.0	4.12	0.0
adiabatic	2.85	2.50			
<sup>1</sup> B <sub>1</sub> , vert	4.99	4.77	0.0515	4.84	0.0193
adiabatic	4.78	4.50			
<sup>2</sup> <sup>1</sup> A <sub>1</sub> , vert	6.36	6.28	0.0160	6.36	0.0010
adiabatic	5.99	5.91			
<sup>1</sup> B <sub>2</sub> , vert	6.78	6.73	0.0029	6.72	1.6 × 10 <sup>-5</sup>
adiabatic	6.40	6.35			

<sup>a</sup> Excitation energies are given relative to the <sup>1</sup>A<sub>1</sub> state. <sup>b</sup> Excitation energies are given relative to the <sup>1</sup>A' state. <sup>c</sup> Excitation energies are given relative to the <sup>1</sup><sup>3</sup>B state. <sup>d</sup> Excitation energies are given relative to the <sup>1</sup>A<sub>1</sub> state.

factors for individual transitions.<sup>51</sup> Scaled by 0.9,<sup>51</sup> CIS/6-311+G(d,p) vibrational frequencies (shown in Table S2 of the Supporting Information) in conjunction with the MRCI+D adiabatic excitation energies were used to calculate the peak positions. The theoretical spectra are shown in Figure 9. In the <sup>1</sup>B<sub>1</sub> state, the H<sub>2</sub>C–C bond is stretched from 1.32 to 1.44 Å and the second CC bond is shortened from 1.29 to 1.21 Å. As a result, two a<sub>1</sub> normal modes are displaced,  $\nu_7$  (2043 cm<sup>-1</sup> in the ground state and 1887 cm<sup>-1</sup> in the excited state) with  $\Delta Q_7 = 0.48$  Bohr·amu<sup>1/2</sup> and  $\nu_5$  (1147 cm<sup>-1</sup> in <sup>1</sup>A<sub>1</sub> and 1112

cm<sup>-1</sup> in <sup>1</sup>B<sub>1</sub>) with  $\Delta Q_5 = 0.15$  Bohr·amu<sup>1/2</sup>. A b<sub>1</sub> mode  $\nu_1$  is strongly distorted, from 233 cm<sup>-1</sup> in <sup>1</sup>A<sub>1</sub> to 433 cm<sup>-1</sup> in the excited state. Comparison between the experimental and calculated positions of the peaks is given in Table 3, and the agreement is good. The spectrum looks like a combination of two vibrational progressions, a more intense one with the spacing of 1887 cm<sup>-1</sup> and a less intense one with the spacing of 900–1000 cm<sup>-1</sup>. In the <sup>2</sup><sup>1</sup>A<sub>1</sub> state, both CC bonds are stretched. The  $\nu_5$  and  $\nu_7$  normal modes are displaced by 0.62 and 0.34 Bohr·amu<sup>1/2</sup>, respectively. The distortion of  $\nu_1$  is less significant. Two vibrational progressions with the spacing of 1704 and 956 cm<sup>-1</sup> appear in the spectrum. In general, our

(51) (a) Mebel, A. M.; Chen, Y. T.; Lin, S. H. *Chem. Phys. Lett.* **1996**, 258, 53. (b) Mebel, A. M.; Chen, Y. T.; Lin, S. H. *J. Chem. Phys.* **1996**, 105, 9007.

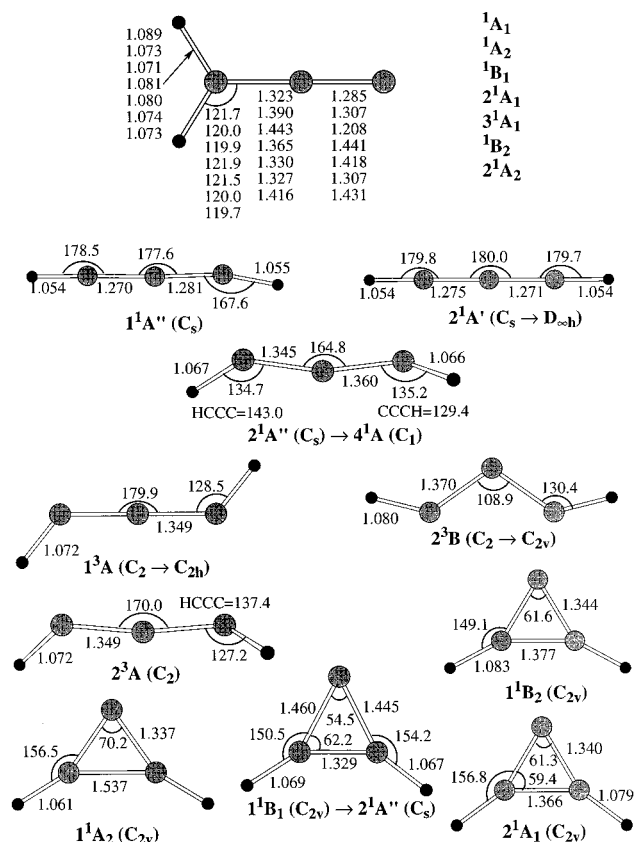


**Figure 8.** CASSCF(8,10)/6-311+G(d,p) optimized geometry of excited states of  $C_3H_2$ .

assignment is close to that proposed by Stanton et al.<sup>19</sup> MRCI energies are more accurate than the EOM-CCSD ones, while the EOM-CCSD vibrational frequencies for the excited states should be more precise than the CIS frequencies.

**(b) Singlet and Triplet Propargylene.** Excitation energies for the singlet and triplet HCCCH are presented in Table 2. All the optimized structures of excited states, discussed below, have all real frequencies at the CIS level. For the singlet, which has a  $C_s$  geometry in the lowest state, the first excited state is  $1^1A''$ . The vertical energy is only 1.17 eV and the transition is weak. At the optimized geometry of  $1^1A''$ , the CC bond lengths become close to each other and the CH bonds are shortened. The adiabatic excitation energy is as low as 0.37 eV. The  $1^1A'$  and  $1^1A''$  potential energy surfaces nearly cross in the vicinity of the equilibrium structure of  $1^1A''$ . The second singlet excited state is  $2^1A'$  with the vertical energy of 2.79 eV. The  $1^1A' \rightarrow 2^1A'$  transition should be stronger than  $1^1A' \rightarrow 1^1A''$ , with the oscillator strength of 0.01. Optimization of  $2^1A'$  gives a nearly linear  $D_{\infty h}$  structure with the CC and CH bonds similar to those in  $1^1A''$ . The adiabatic excitation energy of  $2^1A'$  is predicted to be 1.00 eV. The third state is  $2^1A''$  (3.32 eV). Upon optimization, this state loses symmetry and becomes  $4^1A$  in terms of the  $C_1$  point group. The CC bonds in  $4^1A$  are stretched to 1.35–1.36 Å and the molecule is significantly bent and twisted. The energy of  $4^1A$  with respect to the lowest singlet  $1^1A'$  is 3.05 eV. As seen in Table 2, we calculated vertical excitation energies for several more excited singlet states in the region up to  $\sim 7.3$  eV. Of those, the most intense transitions are expected to be due to  $1^1A' \rightarrow 3^1A'$  (the energy is 5.68 eV and the oscillator strength is 0.01) and  $1^1A' \rightarrow 5^1A'$  (6.33 eV, 0.02).

For triplet HCCCH, the first excited state is  $3^3A$ , 4.10 eV above  $3^3B$  at the geometry of the latter. The oscillator strength for the  $3^3B \rightarrow 3^3A$  transition is  $\sim 0.02$ . Geometry optimization for the

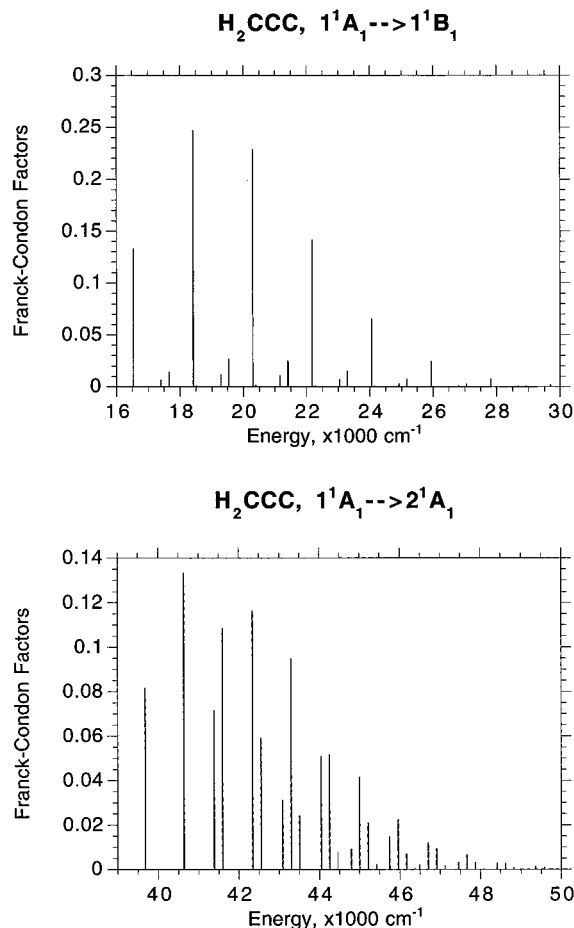


**Figure 9.** Calculated vibronic spectra of  $H_2CCC$  due to the  $1^1A_1 \rightarrow 1^1B_1$  and  $1^1A_1 \rightarrow 2^1A_1$  electronic transitions.

$3^3A$  state gives a structure of nearly  $C_{2h}$  symmetry, shown in Figure 8. The molecule is planar with a linear CCC fragment. The CC bonds are stretched from 1.29 to 1.35 Å and the CCH angles decrease from  $158^\circ$  in  $3^3B$  to  $129^\circ$  in  $3^3A$ . The adiabatic excitation energy is calculated to be 3.28 eV. The difference between the adiabatic and vertical excitation energies is 0.82 eV because of the significant geometry change in  $3^3A$ . The second excited state,  $2^3B$ , has the vertical and adiabatic excitation energies of 4.33 and 3.02 eV. The optimized geometry of  $2^3B$  is also planar, but of  $C_{2v}$  symmetry. The CCC fragment is strongly bent ( $109^\circ$ ) and the CCC bonds are stretched to 1.37 Å. The calculated oscillator strength is as low as 0.0004. For third triplet excited state,  $2^3A$ , the optimized geometry is characterized by the elongation of the CC bonds and bending the CCH fragments, similar to those in  $3^3A$ . Otherwise, the CH bond lengths, the CCC angle, and the HCCC dihedral angles remain close to those in the ground  $3^3B$  state. The vertical excitation energy for  $2^3A$  and the oscillator strength are 5.41 eV and 0.002, respectively. At the CASSCF(8,10)/6-311+G(d,p) level, the adiabatic energy of  $2^3A$  is 0.54 eV lower than the vertical energy. The MRCI+D calculation at the CASSCF optimized geometry, which required the use of a larger active space, 6 electrons on 9 orbitals, gives the energy  $\sim 0.30$  eV lower than the vertical MRCI+D(6,9) energy of  $2^3A$ . Thus, the adiabatic excitation energy of the  $2^3A$  state is predicted to be 5.11 eV (243 nm).

The broad weak absorption band observed in the UV spectra of triplet propargylene<sup>18</sup> between 275 and 350 nm (3.54–4.51 eV) apparently is due to the  $3^3B \rightarrow 3^3A$  and  $3^3B \rightarrow 2^3B$  electronic transitions. The bands lying between 260 (4.77 eV) and 231

**Table 3.** Calculated and Experimental Peak Positions (cm<sup>-1</sup>) in the Vibronic Spectra of H<sub>2</sub>CCC

<sup>1</sup> A <sub>1</sub> → <sup>1</sup> B <sub>1</sub>			<sup>1</sup> A <sub>1</sub> → 2 <sup>1</sup> A <sub>1</sub>		
assign	theoretical peak	exptl band <sup>a</sup>	assign	theoretical peak	exptl band <sup>a</sup>
origin	16534	16611	origin	39682	38810–39682
		16949	5 <sub>0</sub> <sup>1</sup>	40638	40650
1 <sub>0</sub> <sup>2</sup>	17400	17483	7 <sub>0</sub> <sup>1</sup>	41386	
5 <sub>0</sub> <sup>1</sup>	17646	17699	5 <sub>0</sub> <sup>2</sup>	41594	41667
7 <sub>0</sub> <sup>1</sup>	18415	18692	7 <sub>0</sub> <sup>1</sup> 5 <sub>0</sub> <sup>1</sup>	42342	
7 <sub>0</sub> <sup>1</sup> 1 <sub>0</sub> <sup>2</sup>	19281		5 <sub>0</sub> <sup>3</sup>	42550	42373
7 <sub>0</sub> <sup>1</sup> 5 <sub>0</sub> <sup>1</sup>	19527	19685	7 <sub>0</sub> <sup>2</sup>	43090	
7 <sub>0</sub> <sup>2</sup>	20296	20833	7 <sub>0</sub> <sup>1</sup> 5 <sub>0</sub> <sup>2</sup>	43298	43290
7 <sub>0</sub> <sup>2</sup> 1 <sub>0</sub> <sup>2</sup>	21162		5 <sub>0</sub> <sup>4</sup>	43506	
7 <sub>0</sub> <sup>2</sup> 5 <sub>0</sub> <sup>1</sup>	21408	21834	7 <sub>0</sub> <sup>2</sup> 5 <sub>0</sub> <sup>1</sup>	44046	44053
7 <sub>0</sub> <sup>3</sup>	22177	22936	7 <sub>0</sub> <sup>1</sup> 5 <sub>0</sub> <sup>3</sup>	44254	
7 <sub>0</sub> <sup>3</sup> 1 <sub>0</sub> <sup>2</sup>	23043		5 <sub>0</sub> <sup>5</sup>	44462	
7 <sub>0</sub> <sup>3</sup> 5 <sub>0</sub> <sup>1</sup>	23289	23923	7 <sub>0</sub> <sup>3</sup>	44794	
7 <sub>0</sub> <sup>4</sup>	24058	25000	7 <sub>0</sub> <sup>2</sup> 5 <sub>0</sub> <sup>2</sup>	45002	45045
7 <sub>0</sub> <sup>4</sup> 1 <sub>0</sub> <sup>2</sup>	24924		7 <sub>0</sub> <sup>1</sup> 5 <sub>0</sub> <sup>4</sup>	45210	
7 <sub>0</sub> <sup>4</sup> 5 <sub>0</sub> <sup>1</sup>	25170		5 <sub>0</sub> <sup>6</sup>	45418	
7 <sub>0</sub> <sup>5</sup>	25939	26178	7 <sub>0</sub> <sup>3</sup> 5 <sub>0</sub> <sup>1</sup>	45750	
7 <sub>0</sub> <sup>6</sup>	27820		7 <sub>0</sub> <sup>2</sup> 5 <sub>0</sub> <sup>3</sup>	45958	45872
			7 <sub>0</sub> <sup>1</sup> 5 <sub>0</sub> <sup>5</sup>	46166	
			5 <sub>0</sub> <sup>7</sup>	46374	
			7 <sub>0</sub> <sup>4</sup>	46498	
			7 <sub>0</sub> <sup>3</sup> 5 <sub>0</sub> <sup>2</sup>	46706	
			7 <sub>0</sub> <sup>2</sup> 5 <sub>0</sub> <sup>4</sup>	46914	46948

<sup>a</sup> From ref 19.

nm (5.37 eV) can be assigned to the 2<sup>3</sup>A state, although some contribution from 2<sup>3</sup>B cannot be excluded. The next two transitions, <sup>3</sup>B → 3<sup>3</sup>B (5.59 eV) and <sup>3</sup>B → 4<sup>3</sup>B (6.76 eV), are very weak.

**(c) Cyclopropenylidene.** For cyclic C<sub>3</sub>H<sub>2</sub>, the lowest singlet excited state is <sup>1</sup>A<sub>2</sub>, with the vertical excitation energy of 3.92 eV. The <sup>1</sup>A<sub>1</sub> → <sup>1</sup>A<sub>2</sub> transition is symmetry-forbidden. Therefore, only weak absorption due to vibronic coupling might be observed for cyclopropenylidene in the region of ~316 nm. The optimized geometry of the <sup>1</sup>A<sub>2</sub> state is quite different from that of the ground state. It is characterized by two short CC bonds (1.34 Å) and one long CC bond (1.54 Å) between two CH fragments. The electronic structure of <sup>1</sup>A<sub>2</sub>, described earlier by Bofill et al.,<sup>13p</sup> defines the geometric structure: one unpaired electron is located on the p<sub>σ</sub> orbital of the top (hydrogen-less) carbon and three electrons form a π-system of the ring. The second unpaired π-electron is shared by the C(H) atoms. Due to the large geometry change, the adiabatic excitation energy of <sup>1</sup>A<sub>2</sub> is 1.42 eV lower than the vertical energy. At the CIS level, the <sup>1</sup>A<sub>2</sub> optimized structure has no imaginary frequencies.

The second excited state is <sup>1</sup>B<sub>1</sub>, with the calculated vertical energy and the oscillator strength of 4.77 eV and 0.05, respectively. The geometry changes in <sup>1</sup>B<sub>1</sub> are small: the CC(H) bonds are slightly (0.02–0.04 Å) elongated, while the CH bonds are shortened by ~0.01 Å. At the CIS level, the C<sub>2v</sub> optimized geometry has one imaginary frequency of b<sub>2</sub> symmetry (in-plane). Therefore, we carried out the CASSCF optimization within C<sub>s</sub> symmetry for the 2<sup>1</sup>A'' state. The optimization converged to a slightly distorted C<sub>2v</sub> structure. According to Bofill et al.,<sup>13p</sup> the <sup>1</sup>B<sub>1</sub> state has two unpaired electrons on the p<sub>σ</sub> and p<sub>π</sub> orbitals of the top carbon. The

adiabatic excitation energy of <sup>1</sup>B<sub>1</sub> is 4.50 eV. The absorption band for cyclopropenylidene, observed by Seburg et al. in the 270–260 nm (4.59–4.77 eV) region,<sup>18</sup> is due to the <sup>1</sup>A<sub>1</sub> → <sup>1</sup>B<sub>1</sub> transition. The assignment of individual vibronic bands for the <sup>1</sup>B<sub>1</sub> state requires higher level calculations of vibrational frequencies of the excited state followed by the computations of Franck–Condon factors.

The electronic structure of <sup>1</sup>B<sub>2</sub> is similar to that of <sup>1</sup>A<sub>2</sub>, but one of the unpaired electrons is located on the p<sub>π</sub> orbital of the top C. The (H)C–C(H) bond in the optimized structure is 0.05 Å longer than that in <sup>1</sup>A<sub>1</sub> and 0.16 Å shorter than that in <sup>1</sup>A<sub>2</sub>. The other two CC bonds are similar to those in the <sup>1</sup>A<sub>2</sub> optimized structure. The vertical and adiabatic excitation energies for the <sup>1</sup>B<sub>2</sub> state are calculated to be 6.73 and 6.35 eV, and the oscillator strength for the <sup>1</sup>A<sub>1</sub> → <sup>1</sup>B<sub>2</sub> transition is ~0.003. The 2<sup>1</sup>A<sub>1</sub> state has the lone pair of the top carbon atom shifted from the p<sub>σ</sub> to p<sub>π</sub> orbital. 2<sup>1</sup>A<sub>1</sub> is similar to the <sup>1</sup>B<sub>2</sub> state by the geometry and its vertical and adiabatic excitation energies are ~0.4 eV lower than those for <sup>1</sup>B<sub>2</sub>. The <sup>1</sup>A<sub>1</sub> → 2<sup>1</sup>A<sub>1</sub> transition, with the oscillator strength of 0.016, is expected to be stronger than <sup>1</sup>A<sub>1</sub> → <sup>1</sup>B<sub>2</sub>.

The excitation energies of cyclopropenylidene obtained here are significantly lower than the values calculated by Bofill et al. at the CISD/6-31G level.<sup>13p</sup> Comparison of the MRCI+D and EOM-CCSD vertical excitation energies shows that in most cases the EOM-CCSD method performs fairly well. However, there are several obvious failures, such as for the 2<sup>1</sup>A' and 2<sup>1</sup>A'' states of propargylene and some higher excited states of vinylidenecarbene.

**Dissociation of C<sub>3</sub>H<sub>2</sub>.** As seen from the previous section, various isomers of C<sub>3</sub>H<sub>2</sub> can absorb a 193 nm photon. After internal conversion into the ground electronic state, C<sub>3</sub>H<sub>2</sub> can dissociate by numerous pathways discussed below. H<sub>2</sub> elimination from H<sub>2</sub>CCC produces C<sub>3</sub> with the energy loss of 59.8 kcal/mol. The reaction proceeds via transition state TS11 with the barriers of 85.4 and 25.6 kcal/mol in the forward and reverse directions, respectively. The barrier for the 1,1-insertion of H<sub>2</sub> into C<sub>3</sub> is much higher than that for the insertion of H<sub>2</sub>CCC. This result is related to the exothermicities of insertion, 59.8 kcal/mol for C<sub>3</sub> + H<sub>2</sub> and 83.0 kcal/mol for H<sub>2</sub>CCC + H<sub>2</sub>. Considering the elimination reaction, TS11 is an earlier transition state compared to TS2. The HH distance in TS11 is 0.11 Å longer than that in TS2, while the breaking CH bonds are significantly shorter. The CCC bending is similar in the two transition states. H atom elimination from vinylidenecarbene gives linear HCCC. The CH bond dissociation energy in H<sub>2</sub>CCC is found to be 89.3 kcal/mol.

Singlet propargylene can also eliminate molecular hydrogen and form C<sub>3</sub>. The endothermicity of the HCCCH → C<sub>3</sub> + H<sub>2</sub> reaction is 49.4 kcal/mol. The corresponding transition state, TS12, has a peculiar five-member-ring structure of C<sub>2v</sub> symmetry. Both C<sub>3</sub> and H<sub>2</sub> fragments are strongly distorted as compared to the free molecules. The HH bond is stretched by 0.16 Å, the CC bonds are lengthened by 0.05 Å, and the CCC angle is 88.8° vs 180° in C<sub>3</sub>. Meanwhile, the energy of TS12, 84.3 and 73.9 kcal/mol relative to H<sub>2</sub>CCC and HCCCH, respectively, is very close to the energy of TS11. As a result, the activation energies of the 1,3- and 1,1-insertion of C<sub>3</sub> into H<sub>2</sub> are nearly identical. To get some insight in this surprising result, we decomposed the relative energies of the transition states with respect to C<sub>3</sub> + H<sub>2</sub> into three components, distortion of the fragments and their repulsion:

$$E^{\#} = E_{\text{dist}}(\text{C}_3) + E_{\text{dist}}(\text{H}_2) + E_{\text{rep}}(\text{C}_3\text{--H}_2)$$

**Table 4.** Energetics of Various Primary and Secondary Photodissociation Channels of Allene and Propyne and Translational Energy Distribution (kcal/mol)

reaction	$\Delta H$	translational energy <sup>a</sup>			$E^\ddagger$	frag dist		$E_{\text{rep}}$
		min	most prob	max		C <sub>3</sub> H <sub>n</sub>	H <sub>2</sub>	
primary channels								
H <sub>2</sub> CCCH <sub>2</sub> → H <sub>2</sub> CCC + H <sub>2</sub>	83.0	5	20	35	9.4	0.5	2.0	6.9
H <sub>2</sub> CCCH <sub>2</sub> → H <sub>2</sub> CCCH + H	87.8	0	5	34	0.0			
H <sub>3</sub> CCCH → HCCCH + H <sub>2</sub>	94.3	(5) <sup>b</sup>			6.3	1.0	0.5	4.8
H <sub>3</sub> CCCH → H <sub>2</sub> CCC + H <sub>2</sub>	83.9	(0) <sup>b</sup>			43.2	30.3	17.9	-6.0
H <sub>3</sub> CCCH → H <sub>3</sub> CCC + H	130.5	(0) <sup>b</sup>			0.0			
H <sub>3</sub> CCCH → H <sub>2</sub> CCCH + H	88.7	(0) <sup>b</sup>			0.0			
secondary channels								
H <sub>2</sub> CCCH → CCCH + H <sub>2</sub>	84.5	8	40	64	10.4	0.8	2.3	7.3
H <sub>2</sub> CCCH → H <sub>2</sub> CCC + H	96.3	0	12	80	0.0			
H <sub>2</sub> CCCH → HCCCH + H	94.2	(0) <sup>b</sup>			0.0			
C <sub>3</sub> H <sub>3</sub> → C <sub>2</sub> H <sub>2</sub> + CH	77.4	0	4	50	0.0			
H <sub>3</sub> CCC → CCCH + H <sub>2</sub>	42.7	(20) <sup>b</sup>			25.3	2.6	2.8	19.9
H <sub>3</sub> CCC → H <sub>2</sub> CCC + H	54.5	(0) <sup>b</sup>			0.0			
H <sub>2</sub> CCC → C <sub>3</sub> + H <sub>2</sub>	59.8	(15) <sup>b</sup>			25.6	0.2	10.0	15.4
H <sub>2</sub> CCC → HCCC + H	89.3	(0) <sup>b</sup>			0.0			
HCCCH → C <sub>3</sub> + H <sub>2</sub>	49.3	4	32	65	24.5	11.8	8.2	4.5
HCCCH → HCCC + H	78.9	(0) <sup>b</sup>			0.0			
C <sub>3</sub> H <sub>2</sub> → C <sub>2</sub> H + CH	131.6	0	4	60	0.0			
C <sub>3</sub> H <sub>2</sub> → C <sub>2</sub> H <sub>2</sub> + C	135.8	0	6	120	0.0			

<sup>a</sup> From ref 1. <sup>b</sup> Theoretical prediction.

The fragment distortion energies were calculated at the B3LYP level and  $E_{\text{rep}}$  was obtained by subtraction of the distortion energies from the barrier height. For TS11,  $E_{\text{dist}}(\text{C}_3) = 0.2$ ,  $E_{\text{dist}}(\text{H}_2) = 10.0$ , and  $E_{\text{rep}} = 15.4$  kcal/mol. For TS12, C<sub>3</sub> is strongly distorted and  $E_{\text{dist}}(\text{C}_3) = 11.8$  kcal/mol, the distortion of H<sub>2</sub> is slightly lower than that in TS11 (8.2 kcal/mol), and the repulsion energy is only 4.5 kcal/mol. The higher distortion of C<sub>3</sub> in TS12 is compensated by the lower repulsion energy of the fragments. Elimination of a hydrogen atom from propargylene is endothermic by 78.9 kcal/mol.

For the most stable cyclic isomer of C<sub>3</sub>H<sub>2</sub>, we could not find a transition state for H<sub>2</sub> elimination. Formation of C<sub>3</sub> from cyclopropenylidene has to proceed via isomerization to H<sub>2</sub>CCC or HCCCH. H atom splitting from the cyclic C<sub>3</sub>H<sub>2</sub> gives the cyclic C<sub>3</sub>H. The CH bond dissociation energy is calculated to be 100.8 kcal/mol.

Dissociation of propargylene can produce C<sub>2</sub>H + CH and the reaction is endothermic by 131.6 and 144.2 kcal/mol for the singlet and triplet HCCCH, respectively. Cyclopropenylidene can eliminate the hydrogen-less carbon atom giving acetylene. If the reaction proceeds within the singlet manifold, it is calculated to be 136.8 kcal/mol endothermic. The energy of the H<sub>2</sub>CCC → CH<sub>2</sub> (<sup>1</sup>A<sub>1</sub>) + C<sub>2</sub> (<sup>1</sup>Σ<sub>g</sub><sup>+</sup>) reaction is 162.9 kcal/mol. We expect that C<sub>3</sub>H<sub>2</sub> → C<sub>3</sub> + H<sub>2</sub> should be the major channel of dissociation of C<sub>3</sub>H<sub>2</sub> on the ground state surface because it has the lowest activation energy. The other product channels, such as experimentally observed C<sub>3</sub>H<sub>2</sub> → C<sub>2</sub>H + CH and C<sub>3</sub>H<sub>2</sub> → C<sub>2</sub>H<sub>2</sub> + C, as well as C<sub>3</sub>H<sub>2</sub> → C<sub>3</sub>H + H, require higher activation energies. Interestingly, the three C<sub>3</sub>H<sub>2</sub> dissociation product channels observed in the photolysis of allene,<sup>1</sup> C<sub>3</sub> + H<sub>2</sub>, C<sub>2</sub>H + CH, and C<sub>2</sub>H<sub>2</sub> + C, are originated from different isomers, indicating that isomerization of C<sub>3</sub>H<sub>2</sub> plays an important role in the photodissociation dynamics.

**Comparison of the Photodissociation Dynamics of Allene and Propyne.** To fully understand the photodissociation dynamics of C<sub>3</sub>H<sub>4</sub> requires both electronic structure and trajectory or transition state calculations over the full range of the surface explored during the dissociation process. However, the analysis of the ground- and excited-state PES for the C<sub>3</sub>H<sub>n</sub> ( $n = 1-4$ ) species, presented in the previous sections, in

conjunction with the available experimental data, such as the translational energy distribution  $P(E_T)$  curves,<sup>1</sup> allows us to obtain a qualitative insight into the photodissociation mechanism.

In Table 4, we present the theoretical  $\Delta H$  and reverse barrier heights  $E^\ddagger$  for various primary and secondary photodissociation channels of allene and propyne along with the available experimental data on translational energy distribution of the products taken from the  $P(E_T)$  diagrams.<sup>1</sup> From the energy of a photon (193 nm or 148 kcal/mol),  $\Delta H$ , and minimal, maximal, and most probable translational energy one can calculate the minimal, maximal, and most probable values for the internal energies of the products in the primary channels. For instance, for the H<sub>2</sub>CCCH<sub>2</sub> → H<sub>2</sub>CCC + H<sub>2</sub> reaction, the minimal, most probable, and maximal internal energies of the products are estimated to be 30, 45, and 60 kcal/mol. Recent work<sup>52</sup> suggests that the rotational and vibrational distribution of H<sub>2</sub> in this system is similar to the one measured for ethylene. Based on this, we derived the most probable internal energy of H<sub>2</sub>CCC to be ~43 kcal/mol. For a sudden dissociation, conservation of angular momentum limits the rotational energy of H<sub>2</sub>CCC to 1 or 2 kcal/mol. Therefore, the most probable value of  $E_{\text{vib}}(\text{H}_2\text{CCC})$  is 41–42 kcal/mol, which is sufficient to overcome the barrier for the rearrangement of vinylidencarbene to cyclopropenylidene. For the H<sub>2</sub>CCCH<sub>2</sub> → H<sub>2</sub>CCCH + H reaction, the minimal, most probable, and maximal  $E_{\text{int}}(\text{H}_2\text{CCCH})$  are 26, 55, and 60 kcal/mol. The  $P(E_T)$  diagrams for the photodissociation of propyne are not available now, but the theoretical data from Table 4 should be helpful for the analysis of the experimental data.<sup>2</sup> The analysis is more complicated for the secondary channels because the primary products already possess some internal energy when they absorb a second photon.

We can also predict the minimal energy threshold on the  $P(E_T)$  curves. If dissociation takes place on the ground-state surface, after clearing the barrier the reaction occurs fast and most of the potential energy, except the internal energy of the fragments, should be transformed into the translational energy. Therefore, the minimal translational energy can be estimated

(52) (a) Cromwell, E. F.; Stolow, A.; Vrakking, J. J.; Lee, Y. T. *J. Chem. Phys.* **1992**, *97*, 4029. (b) Stolow, A. Private communications.

as follows:

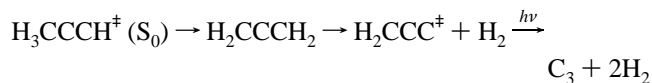
$$E_T(\text{min}) = E^\ddagger - E_{\text{dist}}(\text{fragment 1}) - E_{\text{dist}}(\text{fragment 2}) = E_{\text{rep}}$$

Here,  $E^\ddagger$  is the height of the reverse barrier and  $E_{\text{dist}}$  is the energy of the fragment distortion in the transition state with respect to the free molecule, i.e., the internal energy of the fragment. As seen in Table 4, the calculated fragment repulsion energies  $E_{\text{rep}}$  agree with experimental  $E_T(\text{min})$  where available.

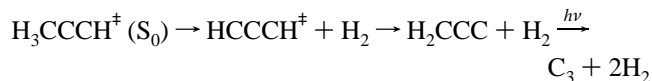
As we discussed earlier,<sup>17</sup> the most likely mechanism for photodissociation of allene at 193 nm to produce  $\text{C}_3\text{H}_2 + \text{H}_2$  involves a Franck–Condon transition to the  $^1\text{B}_1$  excited state. This is followed by a twisting of the  $\text{CH}_2$  groups and then conversion to the vibrationally excited ground state through the seam of crossing. Once the vibrationally excited allene molecule is in the ground electronic state it dissociates to produce  $\text{C}_3\text{H}_2 + \text{H}_2$ . It can also produce  $\text{C}_3\text{H}_3 + \text{H}$ . The atomic hydrogen product channel dominates over the molecular hydrogen channel in both photodissociation<sup>1</sup> and thermal dissociation of allene.<sup>44</sup> This is probably due to the lower activation energy for H elimination (87.8 kcal/mol) compared to  $\text{H}_2$  elimination (92.4 kcal/mol).

After absorption of a second photon,  $\text{C}_3\text{H}_2$  can also undergo internal conversion to the vibrationally excited ground state and then eliminate  $\text{H}_2$  via TS11 or TS12. Because of the low  $E_T(\text{min})$  value, the experimental  $P(E_T)$  diagram for the  $\text{C}_3\text{H}_2 \rightarrow \text{C}_3 + \text{H}_2$  reaction is more consistent with the hypothesis that the  $\text{H}_2$  elimination occurs from HCCCH via TS12, at least partially. This supports our suggestion that  $\text{C}_3\text{H}_2$  has enough internal energy for the isomerization. If the reaction does occur via TS12, the  $\text{C}_3$  molecules will have the bending mode excited. Experiments are currently underway to verify this.

The small amount of  $\text{H}_2$  produced in photodissociation of propyne can be due to isomerization of propyne to allene followed by successive  $\text{H}_2$  eliminations. On the other hand, HCCCH can be produced directly from propyne and it may have the internal energy up to  $\sim 54$  kcal/mol for the case of  $E_T = 0$ . This energy is sufficient for the rearrangement to the other  $\text{C}_3\text{H}_2$  isomers. In both scenarios,



and



the formation of  $\text{C}_3 + \text{H}_2$  from allene and propyne goes via a common intermediate, which gives the identical rotational distribution of the  $\text{C}_3$  products, observed in experiment.<sup>2</sup>

### Concluding Remarks

We have studied potential energy surfaces for various primary and secondary products of the photodissociation of propyne and allene. The calculated heats of the reactions and the activation barriers are expected to be accurate within 1–2 kcal/mol. The theoretical values of  $\Delta H$  and  $E^\ddagger$  are employed to analyze the

experimental translational energy distribution  $P(E_T)$  diagrams, to predict the minimal, maximal, and most probable internal energies of the products, and to estimate the minimal energy threshold on the  $P(E_T)$  curves. The theoretical results for the minimum translational recoil energy agree with those observed experimentally in all cases where there are available data.

The photodissociation of propyne at 193 nm is predicted to involve vertical excitation to the  $^1\text{E}$  electronic state (the vertical energy is 7.31 eV and the adiabatic energies are 5.01–6.62 eV). The fast elimination of the acetylenic hydrogen occurs by traveling along the  $\text{S}_1$  ( $^1\text{A}''$ ) and  $\text{S}_2$  ( $2^1\text{A}'$ ) surfaces followed by a  $\text{S}_2 \rightarrow \text{S}_0$  crossing and dissociation to  $\text{H}_3\text{CCC}$  ( $^2\text{A}_1$ ) + H. A slower dissociation mechanism involves internal conversion into the vibrationally excited ground electronic state. Once the vibrationally excited propyne is on the ground-state PES it dissociates to produce  $\text{H}_2\text{CCCH} + \text{H}$  or  $\text{HCCCH} + \text{H}_2$ , or isomerizes to allene, which, in turn, undergoes the  $\text{H}_2$  elimination giving  $\text{H}_2\text{CCC}$ . The HCCCH produced from propyne can have sufficiently high internal energy to rearrange to  $\text{H}_2\text{CCC}$ . In both cases, the formation of  $\text{C}_3 + \text{H}_2$  from propyne and allene goes via the same intermediate, which explains the identical rotational distribution of the  $\text{C}_3$  products in experiment.

The rearrangement mechanism of  $\text{C}_3\text{H}_2$  and the electronic spectra of various isomers of this species in a broad energy range also have been studied. On the ground-state PES, automerization of  $\text{H}_2\text{CCC}$  can take place either via a cyclopropyne transition state (the barrier is 37.5 kcal/mol)<sup>18</sup> or through isomerization to cyclopropenylidene and backward via TS6 (the barrier is 41.7 kcal/mol). Isomerization of triplet propargylene to cyclo- $\text{C}_3\text{H}_2$  occurs by the ring closure via the crossing seam of the triplet and singlet PES and the activation energy (at MSX1) is predicted to be about 41 kcal/mol. Cyclopropenylidene can undergo automerization by the 1,2-H shift via TS10 with the barrier of 32.4 kcal/mol. The direct triplet HCCCH  $\rightarrow$   $\text{H}_2\text{CCC}$  isomerization (which does not involve cyclo- $\text{C}_3\text{H}_2$ ) proceeds by the 1,3-hydrogen shift via MSX2 and TS8 or TS9 with a high activation energy of 78–81 kcal/mol. The singlet propargylene can also rearrange to cyclo- $\text{C}_3\text{H}_2$  via TS7 (barrier 37.4 kcal/mol) and to  $\text{H}_2\text{CCC}$  via TS8 or TS9. The calculated PES for the ground and excited states allowed us to explain the experimentally observed automerizations and isomerizations of  $\text{C}_3\text{H}_2$  isomers and to assign their UV absorption spectra.

**Acknowledgment.** A.M.M. is grateful to Academia Sinica for his fellowship at IAMS. This work supported in part by the National Science Council of ROC. W.M.J. gratefully acknowledges the support of IAMS for his visiting Professorship position and NASA under Grant No. NAGW-5083. We are thankful to Dr. Q. Cui and Prof. K. Morokuma for providing us the program for the search of MSX.

**Supporting Information Available:** Tables of total energies of various species calculated at the B3LYP/6-311G(d,p) and CCSD(T)/6-311+G(3df,2p) levels, vibrational frequencies of various species, and total energies (hartrees) of various isomers of  $\text{C}_3\text{H}_2$  calculated at the MRCI/ANO(2+) and CCSD/ANO-(2+) levels (5 pages, print/PDF). See any current masthead page for ordering instructions and Web access instructions.